

Peter Julius Waldert

Secure Classification as a Service

Levelled Homomorphic, Post-Quantum Secure Machine Learning Inference
based on the CKKS Encryption Scheme

BACHELOR'S THESIS

Bachelor's degree programmes:
Physics and Information & Computer Engineering

Supervisor

Dipl.-Ing. Roman Walch

Institute of Applied Information Processing and Communications (IAIK)
Graz University of Technology

Graz, July 2022

Abstract

The rapid developments in quantum computation affect cryptography as it is used today. With a sufficiently powerful quantum computer, most digital communication could be decrypted in polynomial time by an eavesdropping party with access to such a potent utility, posing a major problem to the worldwide community. Lattice-based cryptographic schemes aim to mitigate this, while including many further advantages, which will be the main topic of this thesis.

With technological advancements in machine learning, problems long thought to be impossible can now be solved by complicated and resource-intensive neural network structures. Machine learning undoubtedly holds many new possibilities, especially in medicine, although large datasets are especially scarce in this area. **Privacy-Preserving Machine Learning (PPML)** is an emerging field in data science that focusses on leveraging such highly private data anyway, without ever actually seeing it. The techniques behind this are homomorphic encryption schemes, two of which this thesis will discuss in detail.

To demonstrate the possibilities of these homomorphic cryptosystems applied to machine learning inference, a web-based demonstrator for the classification of handwritten digits was developed (confer [figure 1.1](#)). The backend server is written in C++, using the Microsoft **SEAL** homomorphic encryption library. This work starts by introducing the necessary mathematical background, motivating the definitions of the **BFV** and **CKKS** encryption schemes in the following chapter and describing the basics of machine learning along the way. The quantum-mechanical principles and implications of SHOR's algorithm are discussed, further inciting the need for studying the hardness of the **LWE**-based cryptosystems. The final chapters then focus on implementation aspects, the analysis of obtained results and performance benchmarks.

To quickly run the demonstrator on your machine using [Docker](#):

```
1 docker run --name classifier --detach mrp001/sealed-mnist-classifier
2 docker run -p 80:80 -p 443:443 --link classifier mrp001/sealed-mnist-frontend
```

Keywords: FHE, ML, Image Classification, Neural Network, Private AI, PPML, Confidential Computing, Post-Quantum Security

Technologies: Microsoft SEAL (C++, NodeJS), Tensorflow Keras, Numpy, xtensor, Docker, msgpack, WebAssembly, React, Materialize, Nginx

Languages: C++, Python, JavaScript

Contents

1	Introduction	5
2	Background	7
2.1	Polynomial Rings and Modular Arithmetic	7
2.1.1	Cyclotomic Polynomials	10
2.2	Lattice Cryptography	13
2.2.1	Learning with Errors (LWE)	15
2.2.2	Learning with Errors on Rings (RLWE)	16
2.3	Machine Learning	17
2.3.1	Gradient Descent	18
2.3.2	Multi-Layered Neural Networks	19
2.4	Post-Quantum Security	21
2.4.1	Shor's Algorithm	23
2.4.2	Outlook	24
3	Homomorphic Encryption	25
3.1	Homomorphic Encryption using RSA	25
3.2	Gentry's FHE-Scheme and BGV	26
3.3	The BFV Scheme	27
3.3.1	Scheme Definition	27
3.3.2	Verification of the Additive Homomorphism	29
3.4	The CKKS Scheme	30
3.4.1	Encoding and Decoding	30
3.4.2	Scheme Definition	33
3.4.3	Verification of the Additive Homomorphism	34
4	Implementation	36
4.1	Chosen Software Architecture	36
4.2	The MNIST dataset	37
4.3	Our Neural Network	37
4.4	Matrix-Vector Multiplication	39
4.4.1	The Naïve Method	40
4.4.2	The Diagonal Method	41
4.4.3	The Hybrid Method	42
4.4.4	The Babystep-Giantstep Method	44
4.5	Polynomial Evaluation	44
4.6	Further Implementation Challenges	46

5	Results	47
5.1	The Training Process	47
5.2	Accuracy, Precision, Recall	48
5.3	Performance Benchmarks	49
5.4	Ciphertext Visualisations	50
6	Conclusion	51
6.1	Summary	51
6.2	Related Works and Outlook	52
	Acronyms, Definitions and Theorems	53
	Bibliography	55
	List of Figures and Tables	58
A	Supplemental Proofs	59
A.1	Power-of-2 Cyclotomic Polynomials	59
A.2	Babystep-Giantstep Multiplication	60

Chapter 1

Introduction

The most well-known and widely used asymmetric ('public-key') cryptographic scheme, published by the trio RIVEST-SHAMIR-ADLEMAN in 1977 and known as [RSA](#), is based on the hardness assumption of the integer factorisation problem, factorising a large 2-composite number into its two prime factors p and q is believed to be hard ([R. L. Rivest, Shamir and L. M. Adleman 1983](#)). As of today, this factorisation problem has not been proven to be in the [Non-deterministic Polynomial time \(NP\)](#) complexity class, yet it is suspected that it might indeed be [NP-complete](#) (i.e. [NP-hard](#) while still being in [NP](#)) when modelled using a traditional Turing machine. Since the advent of quantum computation, this situation changed as a whole with Peter SHOR's algorithm ([Shor 1997](#)), threatening the security of many cryptosystems, for instance [Rivest-Shamir-Adleman \(RSA\)](#) which is still widely used today despite its known problems.

As it stands, lattice-based cryptography presents a solution to a politically and socially problematic situation in which few parties world-wide, with access to a sufficiently powerful quantum computer, may be able to decrypt most of today's digital communication. [Lattice Cryptography](#) is based on other mathematical problems, shown to be sufficiently hard on quantum computers and traditional ones alike, most notably [LWE](#) ([Regev 2005](#)) which this thesis will discuss in detail.

Many new cryptosystems have been developed on top of LWE, two of which this following thesis will focus on specifically: [BFV](#) and [CKKS](#); whose security is still unaffected by efficient quantum algorithms. Yet, it is not only their security prospect that makes these encryption schemes attractive, but primarily their defining [homomorphic](#) property which allows for computations on the encrypted data. A [fully homomorphic encryption](#) scheme was first introduced by Craig GENTRY in 2009, using a bootstrapping approach ([Gentry 2009](#)). The *levelled* homomorphic [Brakerski-Gentry-Vaikuntanathan \(BGV\)](#) encryption scheme is implemented in [Microsoft SEAL 4.0 2022](#) and allows for integer arithmetic, up to a few multiplication 'levels' deep ([Brakerski, Gentry and Vaikuntanathan 2012](#)). The [Brakerski-Fan-Vercauteren \(BFV\)](#) scheme ([Fan and Vercauteren 2012](#); [Brakerski 2012](#)) is highly similar and described in a bit more detail in [section 3.3](#). And finally, building upon concepts introduced in the former, the [Cheon-Kim-Kim-Song \(CKKS\)](#) scheme ([Cheon et al. 2017](#)) allows for approximative floating-point arithmetic that finally facilitates machine-learning applications.

Machine Learning allows a computer to 'learn' from specifically structured data using linear regression or similar methods, and to apply this 'knowledge' to new, unknown inputs. In its simplest form, or even using a multi-layered neural network, this only requires two different operations on numbers (or even better, vectors): addition and multiplication. Using one of the

Homomorphic Encryption (HE) schemes mentioned above and described in [chapter 3](#), both are given and PPML applications are born!

The present thesis not only focusses on theoretical remarks but also includes a publicly available implementation of an HE classification server written in C++, based on the Homomorphic Encryption library Simple Encrypted Arithmetic Library (SEAL) developed by Microsoft Research (*Microsoft SEAL 4.0* 2022), and a compact graphical user interface to interact with. A screenshot of the main functionality is displayed in [figure 1.1](#).

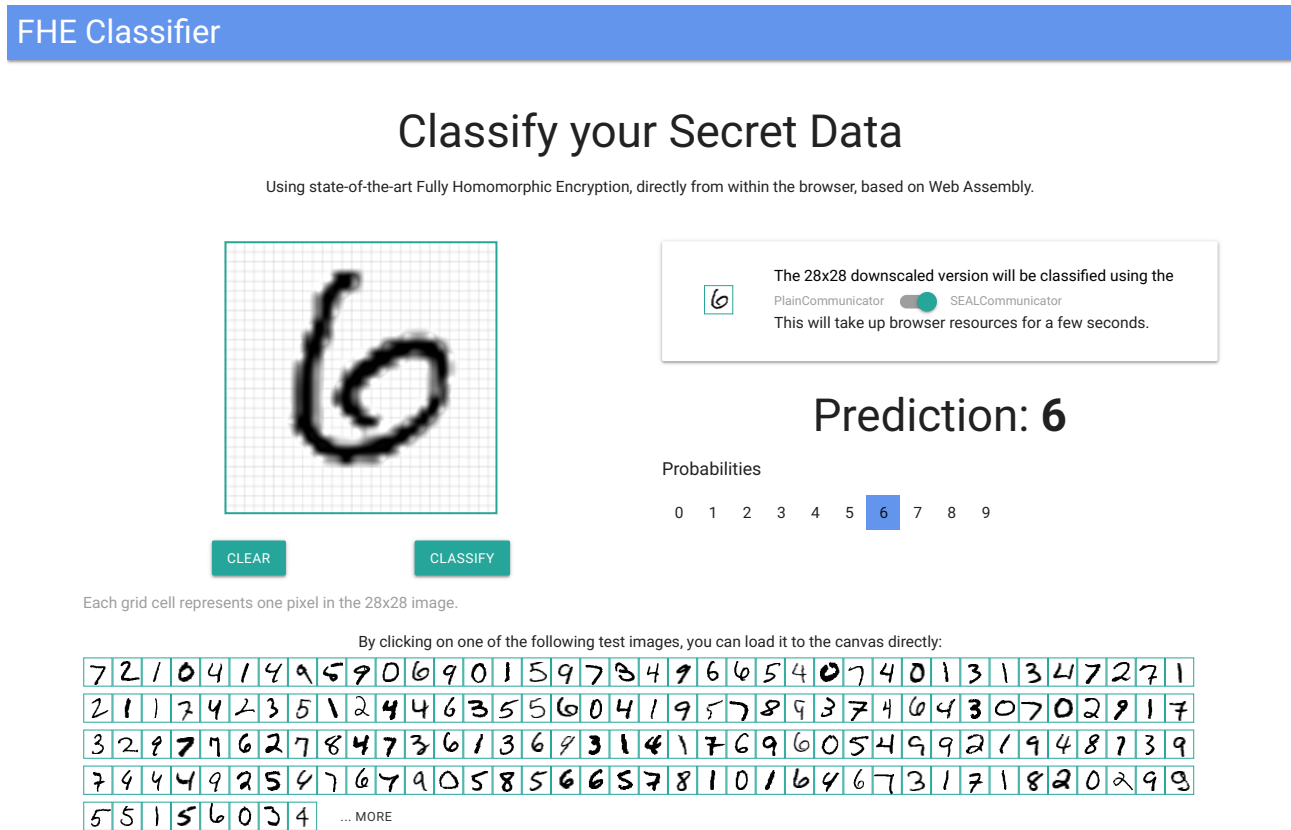


Figure 1.1: The user interface of the demonstrator: users can draw a digit by hand, select one of two communication means (plain or encrypted) and finally let the server handle the classification to obtain a prediction (including a visual of associated probabilities).

The following [chapter 2](#) and [chapter 3](#) aim to introduce most of the necessary theory to understand the HE schemes used in practice today, as well as the simple machine learning approaches involved in securely classifying images as a service.

[Chapter 4](#) then focusses on the concrete system at hand, how the classification of handwritten digits (using the MNIST dataset) works in detail and what challenges arise when dealing with a system which acts not only on plain, but also encrypted data. [Chapter 5](#) analyses the neural network performance in terms of its accuracy, digit-wise precision and recall, documents benchmarks of runtime, message size and accuracy and finally includes a visualisation of the ciphertext (containing all information about the original image).

Chapter 2

Background

The discussion of the HE schemes following in chapter 3 requires some mathematical background that will be introduced here, aiming for a consistent overview rather than full completeness. The last two sections 2.3 and 2.4 introduce some background on Machine Learning and provide an outlook on Quantum Computation and why it affects cryptography today.

Notational Conventions: Let \mathbb{N} denote the natural numbers without 0. For a probability distribution χ over a set R , let sampling a value $x \in R$ from the probability distribution be denoted by $x \leftarrow \chi$. For $a \in \mathbb{R}$ a real number, denote rounding down (floor) a by $\lfloor a \rfloor \in \mathbb{Z}$, rounding up (ceil) by $\lceil a \rceil \in \mathbb{Z}$ and rounding to the nearest integer by $\lfloor a \rceil \in \mathbb{Z}$. Let $[a]_q := a \bmod q$ denote the positive remainder when dividing a by q .

2.1 Polynomial Rings and Modular Arithmetic

As the algebraic structure underlying almost every single symbol following in the next chapters, we recall the definition of a ring:

2.1.1 Definition: Ring

A tuple $(R, +, \cdot)$ consisting of a set R , an addition operation $+$ and a multiplication operation \cdot is referred to as a ring, given that it satisfies the following *ring axioms*:

- Addition is closed: $a + b \in R \quad \forall a, b \in R$.
- Addition is commutative: $a + b = b + a \quad \forall a, b \in R$.
- Addition is associative: $(a + b) + c = a + (b + c) \quad \forall a, b, c \in R$.
- There exists an element $0 \in R$ such that $a + 0 = a \quad \forall a \in R$.
- An additive inverse $-a$ of each element a in R exists, such that $a + (-a) = 0$.
- Multiplication is associative: $(a \cdot b) \cdot c = a \cdot (b \cdot c) \quad \forall a, b, c \in R$.
- Multiplication is closed: $a \cdot b \in R \quad \forall a, b \in R$.
- There exists an element $1 \in R$, referred to as the identity element, or multiplicative identity of R , such that $a \cdot 1 = a \quad \forall a \in R$.
- Multiplication \cdot is distributive w.r.t. addition $+$,
i.e. $a \cdot (b + c) = (a \cdot b) + (a \cdot c) \quad \forall a, b, c \in R$ from the left and
i.e. $(b + c) \cdot a = (b \cdot a) + (c \cdot a) \quad \forall a, b, c \in R$ from the right.

If multiplication is additionally commutative, we refer to the ring as *commutative*:

- Multiplication is commutative: $a \cdot b = b \cdot a \quad \forall a, b \in R$.

Acting as the logical extension of a group, a ring can be considered the intermediary step towards a field (which also defines subtraction and division). Recall that the first 5 properties can be summarised as $(R, +)$ forming an Abelian group. An example of a ring would be the integers themselves, or the integers modulo q : $\mathbb{Z}/q\mathbb{Z}$, sometimes also denoted as \mathbb{Z}_q .

Given two groups $(G, +)$ and a subgroup $(N, +)$, we can construct another group G/N as follows, referred to as a quotient group or factor group:

2.1.2 Definition: Quotient Group / Ring

A quotient group $(G/N, +)$ (pronounced 'G mod N') over the original group G and a normal subgroup N of G with a standard element operation $+$ can be defined using the left cosets

$$g + N := \{g + n \mid n \in N\} \subseteq G$$

of N in G . The corresponding set G/N is defined as

$$G/N := \{g + N \mid g \in G\}$$

whereas the standard operation $+$: $G/N \times G/N \mapsto G/N$ can be extended from the original group G as follows ($g, h \in G$):

$$(g + N) + (h + N) := (g + h)N$$

The quotient set G/N can therefore be identified as the set of all possible left cosets $g + N$ that in union reconstruct the original group G .

As a highly relevant structure to cryptography and a great example of a quotient group, we would like to consider the ring of integers modulo a given modulus $q \in \mathbb{N}$.

2.1.1 Lemma: Ring of Integers Modulo q : $\mathbb{Z}/q\mathbb{Z}$

Using equivalence classes \bar{x}_q modulo q referred to as congruence classes, define the commutative quotient ring of integers modulo q as $(\mathbb{Z}/q\mathbb{Z}, +, \cdot)$ with two operations $+$ and \cdot and

$$\mathbb{Z}/q\mathbb{Z} = \{\bar{x}_q \mid x \in \mathbb{Z}, 0 \leq x < q\}$$

where $q\mathbb{Z} := \{qx \mid x \in \mathbb{Z}\} \triangleleft \mathbb{Z}$ (where \triangleleft refers to the left being a subgroup of the right) denotes the q^{th} multiplicative coset^a of the integers and

$$\bar{x}_q := \{y \equiv x \pmod{q} \mid y \in \mathbb{Z}\}$$

is the set of all multiples of q with remainder x . Note that many operations that resulting groups, rings or fields are commonly equipped with, such as addition or multiplication, propagate to an equivalent definition in the ring of integers modulo q by considering their result as a congruence class instead of it, which in turn is again an element of $\mathbb{Z}/q\mathbb{Z}$.

^afrom the left and from the right, therefore $q\mathbb{Z}$ is called a normal subgroup of \mathbb{Z}

This ring is of specific importance in discrete mathematics and can be regarded as a formalisation of modular arithmetic, much of which we will require at a later point in this chapter.

As a first step towards the first central result, [definition 2.1.7](#), we formally introduce polynomial rings and how to carry out addition and multiplication between them.

2.1.3 Definition: Polynomial Ring over \mathbb{Z}

On the set of all complex-valued polynomials with integer coefficients (a function space)

$$\mathbb{Z}[X] := \left\{ p : \mathbb{C} \mapsto \mathbb{C}, p(x) = \sum_{k=0}^{\infty} a_k x^k, a_k \in \mathbb{Z} \forall k \geq 0 \right\},$$

we can define a commutative ring $(\mathbb{Z}[X], +, \cdot)$ equipped with the standard addition $+$ and multiplication \cdot operations (as an extension over the field \mathbb{C}) of polynomials.

To further elaborate on the polynomial ring operations:

- In their coefficient representations $\mathbf{p} = (p_j)_{j \in \mathbb{N}} = (p_0, p_1, p_2, \dots)$ (which are sequences) and $\mathbf{q} = (q_j)_{j \in \mathbb{N}} = (q_0, q_1, q_2, \dots)$, an addition of two polynomials $p, q \in \mathbb{Z}[X]$ is equivalent to the element-wise addition of their coefficient sequences

$$\begin{aligned} (p + q)(X) &= \sum_{k=0}^{\infty} p_k X^k + \sum_{k=0}^{\infty} q_k X^k = \sum_{k=0}^{\infty} (p_k + q_k) X^k \\ &= \langle (\mathbf{p} + \mathbf{q}), \{X^0, X^1, X^2, \dots\}^T \rangle \end{aligned}$$

which indeed satisfies the additive ring axioms (cf. [definition 2.1.1](#)) due to the existing structure of the underlying field \mathbb{C} .

- The multiplication operation can be defined using a discrete convolution of the coefficient vectors

$$r(X) = (p \cdot q)(X) = \left(\sum_{k=0}^{\infty} p_k X^k \right) \cdot \left(\sum_{l=0}^{\infty} q_l X^l \right) = \sum_{k=0}^{\infty} \sum_{l=0}^{\infty} p_k q_l X^{k+l} = \sum_{k=0}^{\infty} r_k X^k$$

with the arising coefficients $(r_k)_{k \in \mathbb{N}}$ determined by the discrete convolution

$$r_k = \sum_{l=0}^k p_l q_{k-l} \Leftrightarrow \mathbf{r} = \mathbf{p} * \mathbf{q}$$

in this context also referred to as the CAUCHY-product. Therefore,

$$(p \cdot q)(X) = \langle (\mathbf{p} * \mathbf{q}), \{X^0, X^1, X^2, \dots\}^T \rangle.$$

Again, this generally applicable approach satisfies the multiplicative ring axioms and even satisfies commutativity due to the existing structure of the underlying field \mathbb{C} and the symmetry of convolutions.

Where $\langle \cdot, \cdot \rangle$ denotes the dot (scalar) product between two vectors.

Polynomials with degree ≥ 1 over the complex numbers can always be factorised using their roots due to the fundamental theorem of algebra. Polynomials over the integers however, cannot always be factorised further, yielding the definition of an irreducible polynomial.

2.1.4 Definition: Irreducible Polynomials

A polynomial is called irreducible [if and only if \(iff\)](#) it cannot be written as a product of other polynomials *while staying in the same coefficient space*.

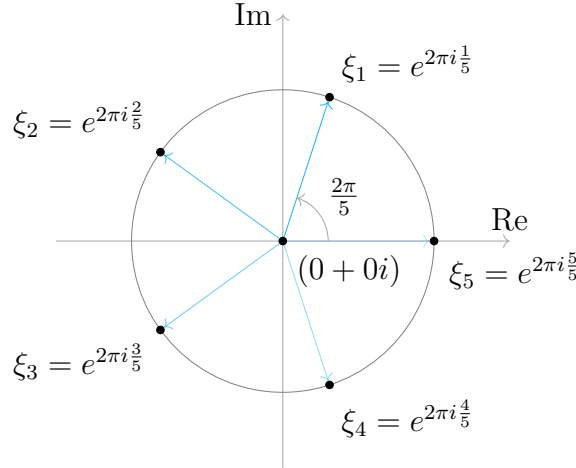


Figure 2.1: The 5th roots of unity visualised on the complex plane. Obviously, they all lie on the unit circle $|z| = 1$, motivating the name of cyclotomic, 'circle-cutting', polynomials, whose roots cut the unit circle into multiple sectors.

2.1.1 Cyclotomic Polynomials

Due to their interesting structure and efficient computability, in the schemes introduced in the following chapter, certain polynomials (definition 2.1.7) are chosen as representations of plaintexts and ciphertexts. An important concept is that of cyclotomic ('circle-cutting') polynomials, which we will discuss in a bit more detail here.

An important polynomial is

$$p : \mathbb{C} \mapsto \mathbb{C}, \quad p(x) = x^n - 1.$$

Its roots, found by solving $p(\xi) = 0$ for ξ , yielding $\xi^n = 1 \leftrightarrow \xi_k = \sqrt[n]{1}$ are referred to as the n^{th} roots of unity, of which there are multiple for each $n \in \mathbb{N}$.

2.1.2 Lemma: The n^{th} roots of unity

For some integer $n \in \mathbb{N}$, the n complex roots $\xi_1, \xi_2, \dots, \xi_n \in \mathbb{C}$ of unity can be found as

$$\xi_k := e^{2\pi i \frac{k}{n}} \quad k \in \{1, 2, \dots, n\}$$

with i being the imaginary unit. Confer figure 2.1. Using EULER's identity, their real and imaginary components can be explicitly found as $\xi_k = \cos\left(2\pi \frac{k}{n}\right) + i \sin\left(2\pi \frac{k}{n}\right)$.

An n^{th} root of unity y is referred to as *primitive*, iff there exists no $m < n$ for which that root y is also an m^{th} root of unity, i.e. $y^m \neq 1$. An equivalent indicator of a primitive root is $\gcd(m, n) = 1$, referring to the greatest common divisor between m and n which is 1 iff they are mutually prime.

Due to the fact that for any $k, l \in \mathbb{Z}$, their product $\xi_k \cdot \xi_l$ is also a root of unity, and $\xi_{k+jn} = \xi_k \forall j \in \mathbb{Z}$, they clearly comprise a cyclic Abelian group over the complex numbers \mathbb{C} under multiplication with (for instance) the first root $\xi_1 = e^{2\pi i \frac{1}{n}}$ as its generator.

2.1.5 Definition: Cyclotomic Polynomial

Given the n^{th} roots of unity $\{\xi_k\}$, we can define the n^{th} cyclotomic polynomial $\Phi_n \in \mathbb{Z}[X]$ as the product over all primitive roots of unity

$$\Phi_n(x) := \prod_{\substack{k=1 \\ \xi_k \text{ primitive}}}^n (x - \xi_k).$$

It is unique for each given $n \in \mathbb{N}$.

The number of primitive roots of unity is given by $\varphi(n)$, denoting EULER's totient function which counts the natural numbers m less than n who do not share a common divisor $\neq 1$, i.e. $\gcd(m, n) = 1$. $\varphi(n)$ therefore also counts the number of primitive roots of unity for n , consequently also yielding the degree of the n^{th} cyclotomic polynomial.

An important aspect of cyclotomic polynomials is that they are irreducible over their coefficient space, the integers \mathbb{Z} .

2.1.1 Remark: Irreducibility of Cyclotomic Polynomials

Cyclotomic polynomials are always irreducible.

This enables us to *uniquely* define a quotient ring with cyclotomic polynomials as moduli, later. In theory, there are multiple equivalent definitions of said ring, but by convention we choose the cyclotomic polynomial because it cannot be simplified further. The proof for [remark 2.1.1](#) is quite cumbersome, but can be found in [Serge 2002](#).

2.1.1 Theorem: $2^{k\text{th}}$ Cyclotomic Polynomial

The M^{th} cyclotomic polynomial, where $M = 2N = 2^k$ ($k \in \mathbb{N}$) is a power of 2, can be identified as

$$\Phi_M(x) = x^N + 1.$$

Its degree is N , consistent with $\varphi(2^k) = 2^{k-1} \forall k \in \mathbb{N}$.

Find a short but illustrative proof of [theorem 2.1.1](#) in [appendix A.1](#).

2.1.6 Definition: Ring of Polynomials of highest degree $N - 1$

For a power-of-2 N , one can construct the quotient ring $(R, +, \cdot)$ as

$$R := \mathbb{Z}[X]/(X^N + 1)$$

where $(X^N + 1)$ denotes the set of all polynomial multiples of the polynomial $p \in \mathbb{Z}[X]$, $p(x) := x^N + 1$, so

$$(X^N + 1) := \{q : \mathbb{C} \mapsto \mathbb{C}, q(x) = r(x) \cdot (x^N + 1) \mid r \in \mathbb{Z}[X]\}.$$

The elements of R are then polynomials with integer coefficients of maximum degree $N - 1$.

If N is a power of 2, according to [theorem 2.1.1](#),

$$R = \mathbb{Z}[X]/\Phi_d(X) = \mathbb{Z}[X]/(X^N + 1)$$

is the set of integer-coefficient polynomials reduced modulo $\Phi_d(X)$, the d^{th} cyclotomic polynomial with $N = \varphi(d) = \frac{d}{2}$. Since every cyclotomic polynomial is irreducible, this is a unique representation of R without any possible further simplifications. Therefore, in the following we will focus on power-of-2 cyclotomic polynomials, which turn out to be even more useful when defining FFT-optimized operations on them.

As promised above, we will require [lemma 2.1.1](#) for the fundamental structure underlying the [HE](#) schemes described in the next chapter, defining ourselves a ring with coefficients in said quotient ring $\mathbb{Z}/q\mathbb{Z}$.

2.1.7 Definition: Polynomial Ring modulo q

Further modifying $R = \mathbb{Z}[X]/(X^N + 1)$ for N a power of 2 to only take coefficients mod q , we obtain two equivalent definitions for the same ring:

$$R_q := R/qR = (\mathbb{Z}/q\mathbb{Z})[X]/(X^N + 1)$$

which contains polynomials with integer coefficients modulo q of degree $N - 1$. Explicitly stated, the set can be written as:

$$R/qR = \{p : \mathbb{C} \mapsto \mathbb{C}, p(x) = \sum_{k=0}^{N-1} a_k x^k \mid a_k \in \mathbb{Z}/q\mathbb{Z}\}$$

This bounded polynomial ring is central to understanding objects in the next chapter and [definition 2.1.7](#) can be regarded as the central result of this section.

2.2 Lattice Cryptography

Lattice-based cryptography takes a different approach to encryption than classical factorisation or the discrete logarithm problem, as it is based on different hardness assumptions, namely ones on [lattice](#) problems. The goal of any mathematical encryption scheme is to leave a potential attacker with a computationally hard, at best infeasible, problem to solve when attempting to decrypt messages without a secret key. This section will start with three basic problems, SVP, GapSVP and SIS and move on to [Learning With Errors \(LWE\)](#) and [Learning With Errors on Rings \(RLWE\)](#). To illustrate the connection of these problems to lattices, we take a closer look at them before considering further details of LWE. Most notably, lattice problems are conjectured to be secure against quantum computers ([Corrigan-Gibbs, S. Kim and Wu 2018](#)).

2.2.1 Definition: Lattice

A lattice $(\mathcal{L}, +, \cdot)$ is a vector field over the integers $(\mathbb{Z}, +, \cdot)$, defined using a set of n basis vectors $\mathbf{b}_1, \mathbf{b}_2, \dots, \mathbf{b}_n \in \mathbb{R}^n$, that can be introduced as a set

$$\mathcal{L} := \left\{ \sum_{i=1}^n c_i \mathbf{b}_i \mid c_i \in \mathbb{Z} \right\} \subseteq \mathbb{R}^n$$

equipped with at least vector addition $+: \mathcal{L} \times \mathcal{L} \mapsto \mathcal{L}$ and scalar multiplication $\cdot: \mathbb{Z} \times \mathcal{L} \mapsto \mathcal{L}$. As an extension of \mathbb{R}^n , the Euclidean norm $\|\cdot\|$ is also defined and the standard Euclidean metric $d: \mathcal{L} \times \mathcal{L} \mapsto \mathbb{R}$, yielding a metric space (\mathcal{L}, d) , can be obtained by the norm of a vector difference, denoted $\|(\cdot) - (\cdot)\|$.

Lattices are a common concept appearing in many areas of mathematics and physics, related to their effective representation as data structures and also geometric intuition (cf. [figure 2.2](#)). Its *minimum distance* λ_{min} is defined as the smallest Euclidean distance between two points $\mathbf{p}_1, \mathbf{p}_2 \in \mathcal{L}$

$$\lambda_{min} := \min_{\mathbf{p}_1, \mathbf{p}_2 \in \mathcal{L}} d(\mathbf{p}_1, \mathbf{p}_2) = \min_{\mathbf{p}_1, \mathbf{p}_2 \in \mathcal{L}} \|\mathbf{p}_1 - \mathbf{p}_2\|,$$

which can be equivalently thought of as the minimal length of any non-zero vector in the lattice \mathcal{L} , because of $\mathbf{0}$ always being an element of the lattice which can be chosen as \mathbf{p}_1 and the translational symmetry between fundamental lattice volumes (or regions).

The three problems frequently showing up in cryptography are stated below, each taking a different approach in their own interesting way.

2.2.2 Definition: Shortest Vector Problem (SVP)

Given a lattice \mathcal{L} constructed from n basis vectors, find the shortest non-zero lattice vector $\mathbf{x} \in \mathcal{L} \setminus \{\mathbf{0}\}$, i.e. find \mathbf{x} such that $\|\mathbf{x}\| = \lambda_{min}$ ([Peikert 2016](#)).

Based on SVP, one can construct GapSVP, an approximative version with advantages for usage in practical problems.

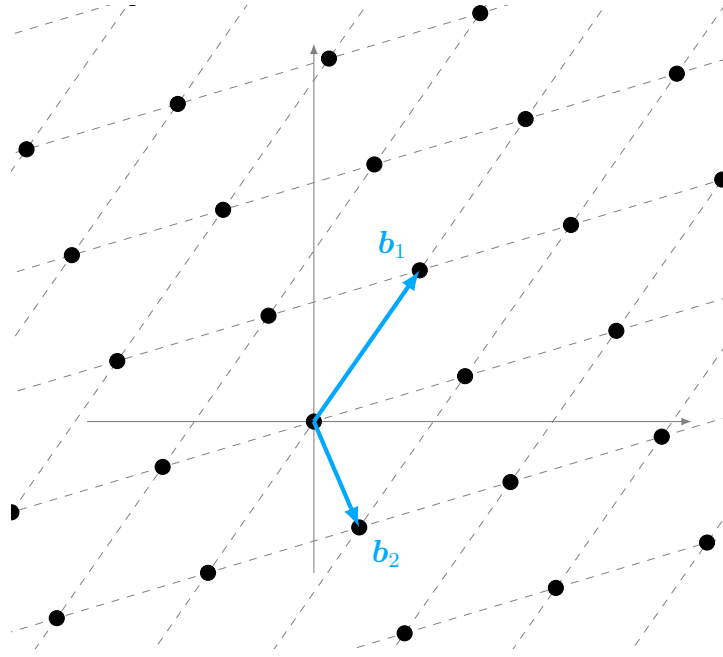


Figure 2.2: Illustration of a standard lattice \mathcal{L} over the integers \mathbb{Z} with two basis vectors \mathbf{b}_1 and \mathbf{b}_2 (cf. [definition 2.2.1](#)). The shortest vector problem in this case is solved by $\mathbf{x} = 0\mathbf{b}_1 \pm 1\mathbf{b}_2$.

2.2.3 Definition: Decisional Approximate SVP (GapSVP)

Given a lattice \mathcal{L} and some pre-defined function $\gamma : \mathbb{N} \mapsto \mathbb{R}$ depending on the lattice dimension n (constant for a given \mathcal{L}) with $\gamma(n) \geq 1$, the decisional approximate shortest vector problem is distinguishing between $\lambda_{\min} \leq 1$ and $\lambda_{\min} > \gamma(n)$. For other cases, it is up to the algorithm what to return.

2.2.4 Definition: Short Integer Solution (SIS) Problem

For m given vectors $(\mathbf{a}_i)_{0 \leq i \leq m} \in (\mathbb{Z}/q\mathbb{Z})^n$ that comprise the columns of a matrix $A \in (\mathbb{Z}/q\mathbb{Z})^{n \times n}$ and an upper bound β , find a solution vector $\mathbf{z} \in \mathbb{Z}^n \setminus \{\mathbf{0}\}$ such that

$$A\mathbf{z} = \mathbf{0} \quad \text{with} \quad \|\mathbf{z}\| \leq \beta.$$

Note that without the last requirement $\|\mathbf{z}\| \leq \beta$, the [Shortest Integer Solution \(SIS\)](#) problem can be easily solved through Gaussian elimination or similar algorithms, however they rarely yield a short (or *the* shortest) solution. It can be shown that solving [SIS](#) is at least as hard as solving the [Decisional Approximate Shortest Vector Problem \(GapSVP\)](#) with appropriate parameters ([Ajtai 1996](#)).

Using the above problems, multiple cryptographic primitives can be constructed due to the proven hardness that also propagates to quantum computers. Examples include collision resistant hash functions, signatures, pseudorandom functions or even Regev's public-key cryptosystem that is based on [LWE](#), which is reduced to the other lattice problems ([Peikert 2016](#)).

2.2.1 Learning with Errors (LWE)

Next, we would like to consider **LWE**, a computing problem that is believed to be sufficiently hard to be used in cryptography and, most notably, is not yet solvable in linear time by a quantum algorithm (cf. [section 2.4](#)), like any other cryptographic lattice problem so far. Its hardness assumptions are related to GapSVP and were first formally proven by [Regev](#), for which he received the 2018 Gödel price.

2.2.5 Definition: LWE-Distribution $A_{\mathbf{s}, \chi_{\text{error}}}$

Given a prime $q \in \mathbb{N}$ and $n \in \mathbb{N}$, we choose some secret $\mathbf{s} \in (\mathbb{Z}/q\mathbb{Z})^n$. In order to sample a value from the LWE distribution $A_{\mathbf{s}, \chi_{\text{error}}}$:

- Draw a random vector $\mathbf{a} \in (\mathbb{Z}/q\mathbb{Z})^n$ from the multivariate uniform distribution with its domain in the integers up to q .
- Given another probability distribution χ_{error} over the integers modulo q , sample a scalar 'error term' $\mu \in \mathbb{Z}/q\mathbb{Z}$ from it, often also referred to as noise.
- Set $b = \mathbf{s} \cdot \mathbf{a} + \mu$, with \cdot denoting the standard vector product.
- Output the pair $(\mathbf{a}, b) \in (\mathbb{Z}/q\mathbb{Z})^n \times (\mathbb{Z}/q\mathbb{Z})$.

The general approach useful to cryptography is to sample an element from the LWE-distribution and construct two problems out of it, *search*-LWE and *decision*-LWE.

2.2.6 Definition: LWE-Problem - Search Version

Given m independent samples $(\mathbf{a}_i, b_i)_{0 \leq i \leq m}$ from $A_{\mathbf{s}, \chi_{\text{error}}}$, find the secret \mathbf{s} .

2.2.7 Definition: LWE-Problem - Decision Version

Given m samples $(\mathbf{a}_i, b_i)_{0 \leq i \leq m}$, distinguish (with non-negligible advantage) whether they were drawn from $A_{\mathbf{s}, \chi_{\text{error}}}$ or from the uniform distribution u over $(\mathbb{Z}/q\mathbb{Z})^n \times (\mathbb{Z}/q\mathbb{Z})$.

In their above definitions, [Regev](#) showed that the two problems are equivalent.

2.2.1 Theorem: Hardness of LWE

If there exists an efficient algorithm that solves either search-LWE or decision-LWE then there exists an efficient algorithm that approximates the decision version of the shortest vector problem (GapSVP) in the worst case ([Regev 2010](#)).

He also provided a construction of a public-key cryptosystem based on them, i.e. an asymmetric cryptographic system for at least two parties that includes a public and corresponding private key.

Public-key cryptosystems are fundamentally different from symmetric systems, which only require one single key for encryption and decryption at the same time, known by all involved parties. Often times, public-key schemes (rather slow) are used to exchange keys for subsequent symmetric encryption (rather fast) of large plaintexts, for instance in the [Transport Layer Security \(TLS\)](#) protocol ([Rescorla 2018](#)).

2.2.2 Learning with Errors on Rings (RLWE)

Similar to [definition 2.2.5](#), the Ring-LWE distribution is derived as follows ([Lyubashevsky, Peikert and Regev 2010](#)):

2.2.8 Definition: RLWE-Distribution $B_{s, \chi_{\text{error}}}$

Given a quotient [ring](#) $(R/qR, +, \cdot)$, we choose some secret $s \in R/qR$. In order to sample a value from the RLWE distribution $B_{s, \chi_{\text{error}}}$:

- Uniformly randomly draw an element $a \in R/qR$
- Given another probability distribution χ_{error} over the ring elements, sample an 'error term' $\mu \in R/qR$ from it, also referred to as noise.
- Set $b = s \cdot a + \mu$, with \cdot denoting the ring multiplication operation.
- Output the pair $(a, b) \in R/qR \times R/qR$.

The search and decision problems can be constructed in the same manner as for [LWE](#):

2.2.9 Definition: RLWE-Search Problem

Given m independent samples $(a_i, b_i)_{0 \leq i \leq m}$ from $B_{s, \chi_{\text{error}}}$, find the secret s .

2.2.10 Definition: RLWE-Decision Problem

Given m samples $(a_i, b_i)_{0 \leq i \leq m}$, distinguish (with non-negligible advantage) whether they were drawn from $B_{s, \chi_{\text{error}}}$ or from the uniform distribution u over $R/qR \times R/qR$.

The main advantage of RLWE over LWE is that is conceptually similar and yet simple to formalise over an arbitrarily chosen [ring](#) $(R, +, \cdot)$ which allows for a vast amount of applications and interesting constructions.

In [LWE](#)-based cryptosystems, the public key consists of m LWE-distribution ([definition 2.2.5](#)) samples of $A_{s, \chi_{\text{error}}}$ hiding the secret s . An attacker would thereby need to solve the LWE-Problem ([definition 2.2.6](#)) in order to retrieve the secret key from the public key, which is highly undesirable for a solid cryptosystem of course, but also hardly feasible with well-chosen parameters, assuming the hardness of the LWE problem (cf. [theorem 2.2.1](#)). For RLWE, the public key only consists of a single RLWE-distribution sample of $B_{s, \chi_{\text{error}}}$ ([definition 2.2.8](#)) which is usually smaller since it is comprised of only two elements in R/qR . Keys are usually smaller in RLWE, depending on the choices of p , q , n and m .

Due to their similarity, RLWE samples can even be translated into equivalent LWE samples. In the case above, a straightforward way is to encode the polynomial coefficients of the RLWE public and secret key into a matrix $A \in (\mathbb{Z}/p\mathbb{Z})^{m \times n}$, vector $\mathbf{b} \in (\mathbb{Z}/p\mathbb{Z})^m$ and vector $\mathbf{s} \in (\mathbb{Z}/p\mathbb{Z})^n$ to arrive at the corresponding LWE keys. A similar approach may be chosen for the relinearisation (and possibly, Galois) keys.

This translation can be used to infer security requirements from LWE (a well-studied problem) over to RLWE to find secure parameters of the cryptosystem.

2.3 Machine Learning

Undoubtedly one of the most prevalent concepts in today's computing world, **Machine Learning (ML)** has shaped how computers think and how we interact with them significantly. As Shafi GOLDWASSER puts it, '*Machine Learning is somewhere in the intersection of Artificial Intelligence, Statistics and Theoretical Computer Science*' (Goldwasser 2018).

Within the scope of this thesis, the basics of neural networks and associated learning methods shall be covered, limited to the category of supervised learning problems (as opposed to unsupervised learning problems). Supervised learning refers to the machine *training* an algorithm to match some input data (features) with corresponding output data (targets), often related to pattern recognition. The trained algorithm can then be utilised to match fresh input data with a prediction of the targets.

A popular subset of applications to **ML** are classification problems, predominantly image classification, which was not as easily possible before without a human eye due to the lack of computing power. Classification problems can be formulated quickly, the goal is to computationally categorize input data (for instance, images) into a predefined set of classes (for instance, cats and dogs). The primary concept behind **Machine Learning** is not at all new, linear regression was already employed by GAUSS and LEGENDRE in the early 19th century; the term 'Neural Network' was coined by MCCULLOCH and PITTS in 1943. Much media attention was earned in the 2000-2010 decade when larger image classification problems became feasible with the increasing computational power of modern computers, up until the advent of Deep Learning (Bishop and Nasrabadi 2007).

2.3.1 Definition: Linear Regression

Given an input vector $\mathbf{x} \in \mathbb{R}^n$, the goal of linear regression is to predict the value of a target $t \in \mathbb{R}$, according to some linear model M .

To illustrate the concept, we will focus on a simple learning method, namely that of gradient descent. In supervised learning problems, this technique first requires us to introduce a loss (error) function $L : \mathbb{R}^n \mapsto \mathbb{R}$, usually **Mean-Squared-Error (MSE)**, which has comparably nice convergence properties due to its parabolic shape:

$$L(\mathbf{w}) := \frac{1}{2} \sum_{i=1}^N (t_i - \mathbf{w}^T \phi(\mathbf{x}_i))^2 = \frac{1}{2} (\mathbf{t} - \Phi \mathbf{w})^T (\mathbf{t} - \Phi \mathbf{w})$$

where $\mathbf{w} \in \mathbb{R}^n$ represents the weights and $\Phi \in \mathbb{R}^{N \times (n+1)}$ is an auxiliary matrix introduced for compact notation, consisting of basis functions $\phi : \mathbb{R}^n \mapsto \mathbb{R}^N$ applied to the inputs \mathbf{x}_i , referred to as the design matrix. This approach allows for a great deal of flexibility when working with more complicated datasets, simply choosing a suitable basis often reduces the problem to a perfectly linear one, easing the fitting process. When $L(\mathbf{w}^*) = 0$, this means we have found the perfect weights, since our predictions exactly match the targets (labels) t_i . This is not always possible, so we aim for the minimum error between predictions and targets. In other words, our goal is to find

$$\mathbf{w}^* = \operatorname{argmin}_{\mathbf{w} \in \mathbb{R}^n} L(\mathbf{w})$$

given a dataset $\{\mathbf{x}_i, t_i\}$.

2.3.1 Gradient Descent

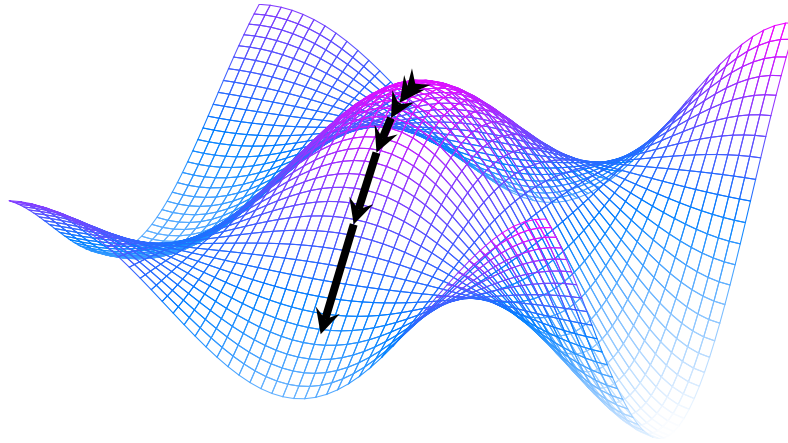


Figure 2.3: An illustration of Gradient Descent on a given loss function $L(w_x, w_y)$ in parameter space (w_x, w_y) , adapted from [StackExchange 2020](#). At each iteration, gradient descent advances in the opposite direction of the gradient $-\nabla L$ to approach a local minimum.

A common method to find such a minimum is **Gradient Descent (GD)**, a straightforward iterative technique to find nearby minima, given a starting position \mathbf{w}_0 in 'parameter space'. In its simplest form, **GD** simply evaluates the *gradient* of the loss function L at the starting point \mathbf{w}_0 , yielding a direction in parameter space in which the loss will increase the most at this given point. Therefore, we advance in the opposite direction given by $-\nabla L$, by a distance η . In the next iteration, our subsequent guess for the local minimum is then given by

$$\mathbf{w}_{i+1} = \mathbf{w}_i - \eta \nabla L$$

which we choose as the next starting point to repeat the process as can be seen in [figure 2.3](#). The iteration finishes when $\|\nabla L\| = 0$ and the Hessian at \mathbf{w}_i is positive definite, indicating a proper minimum, or when a recurring loop in the iteration sequence is detected, or when the loss variation $|L(\mathbf{w}_{i+1}) - L(\mathbf{w}_i)|$ deceeds a given threshold ([Bishop and Nasrabadi 2007](#)).

Note that without modification, **GD** is not a reliable method to find global minima, only local ones. An effective optimisation would be mixing **GD** with Monte-Carlo Markov Chain methods, traversing through parameter space given some probability distribution, and performing **GD** subsequently at multiple locations, thereby escaping the local minima's wells to possibly reach a global minimum. Another useful optimisation is to make the distance η dependent on the iteration step, causing larger jumps in the beginning and smaller ones towards the end - effectively preventing ineffective jump loops around the minimum without approaching the minimum any further.

One of the biggest advantages of **Gradient Descent** is its versatility, given any differentiable loss function, no matter how complicated, at least some progress can be made with **GD**. If the loss function has a simpler form (if it can be written as a quadratic form for instance), and to make up for numerical problems and potentially slow convergence, **GD** can be replaced by more sophisticated methods such as Conjugate Gradient (with convergence guarantees within a certain boundary) or by adding in momentum to the distance travelled in each **GD** iteration ([Bishop and Nasrabadi 2007](#)).

2.3.2 Multi-Layered Neural Networks

As the relations behind data become more and more complicated, the demand for more sophisticated modelling methods increases. Frank ROSENBLATT first implemented the *Perceptron* function invented by MCCULLOCH and PITTS, an object that closely resembles the neural network structures still in use today. The perceptron is a function $\text{Perceptron}_{w,b} : \mathbb{R}^n \mapsto \{0, 1\}$ defined as follows:

$$\text{Perceptron}_{w,b}(\mathbf{x}) := \begin{cases} 1 & \text{if } \mathbf{w} \cdot \mathbf{x} + b > 0, \\ 0 & \text{otherwise} \end{cases}$$

It only has binary output, on which it decides by performing a dot product between the weights vector $\mathbf{w} \in \mathbb{R}^n$ and the input, before adding a bias $b \in \mathbb{R}$ to it. When given a binary target dataset $\{\mathbf{x}_i, t_i\}$, the goal of the training process is to determine the weights \mathbf{w} and bias b such that $\text{Perceptron}_{w,b}(\mathbf{x}_i) = t_i$ for as many samples as possible.

MCCULLOCH and PITTS further employed multiple consecutively connected perceptrons to form a larger 'network', each one referred to as a layer. Neural networks used today are remarkably similar in their structure (cf. figure 2.4). A neural network usually consists of multiple layers of potentially different types, commonly used ones include *Dense* ('Fully Connected') Layers (essentially, matrix multiplication + bias), *Convolutional Layers* (given a kernel, they perform a discrete multivariate convolution over the dataset) and mixtures of non-linear, differentiable, activation functions, max-pooling, etc. in between. Each Dense Layer is usually followed by an activation function such as

$$\begin{aligned} \text{relu}(\mathbf{x}) &:= \max(\mathbf{x}, 0), \\ \text{softmax}(\mathbf{x}) &:= \frac{e^{\mathbf{x}}}{\sum_{i=1}^n e^{x_i}}, \end{aligned}$$

$\tanh(\mathbf{x})$ or $\text{sigmoid}(\mathbf{x})$. They usually play the role of keeping the output bounded and/or sorting for 'activated' values (Bishop and Nasrabadi 2007).

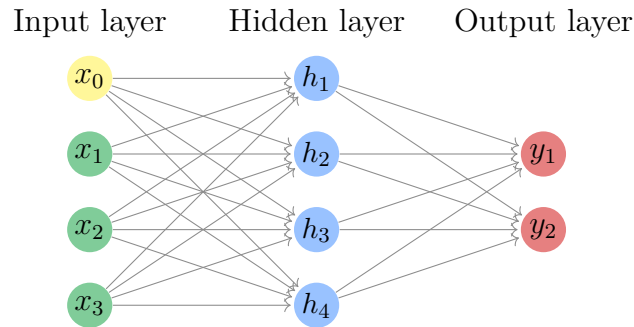


Figure 2.4: A simple neural network resembling the structure we use in our demonstrator, the input (a 784 entry vector) is forwarded to the second layer using $\mathbf{h} = \text{relu}(M_1\mathbf{x} + \mathbf{b}_1)$, resulting in a vector of 128 entries, and finally forwarded to the output layer with $\mathbf{y} = \text{softmax}(M_2\mathbf{h} + \mathbf{b}_2)$. Each of the 10 outputs in \mathbf{y} corresponds to a 'probability' associated with each digit from 0 to 9.

The training process is more complicated in the case of a layered network, especially with non-linear activation functions in between. Yet, the basic principle behind the training process stays the same: Evaluating the loss function L (depending on all weights, biases, convolutional kernels and other parameters in the network) and finding the direction in parameter space in which the loss shrinks, formalised by the layer-wise gradient (for which we require the activation functions to be differentiable). The *Backpropagation Algorithm*, an interactive process similar

to **GD**, does exactly that: Evaluating the gradient of the loss function on the last layer and inversely forwarding the changes to the layer before it, and so on. From there, inferences on the weights, biases and other parameters can be made in order to update them for the next iteration and start over again, repeating the process, working ourselves towards the minimal loss possible (Bishop and Nasrabadi 2007).

As a final note to better understand the implications and possibilities of a large neural network, consider the following universal approximation theorem:

2.3.1 Theorem: Universal Approximation

If the neural network has at least one hidden layer, proper non-linear activation functions and enough data and hidden units, it can approximate any continuous function $y(x, w) : \mathbb{R}^n \mapsto \mathbb{R}$ arbitrarily well on a compact domain (Hornik, Stinchcombe and White 1989).

In the case of our demonstrator, the network consists of two fully connected layers with a Taylor-approximated **relu** activation function in between, which we need to be able to classify on encrypted data. For more details on the implemented neural networks' structure, code and performance, refer to **chapter 4** and **chapter 5**.

An alternative approach to modelling higher dimensional data would be *Gaussian Processes*, a **Machine Learning** technique with a focus on different applications than neural networks', but just as powerful (Mackay 2004, Chapter 45). The mathematical structure behind the model is a multivariate Gaussian distribution

$$p : \mathbb{R}^n \mapsto \mathbb{R}, p(\mathbf{x}) := \frac{1}{\sqrt{(2\pi)^n |\Sigma|}} e^{-\frac{1}{2}(\mathbf{x}-\boldsymbol{\mu})^T \Sigma^{-1}(\mathbf{x}-\boldsymbol{\mu})},$$

in many cases allowing for explicit analytical expressions and calculations as compared to multi-layered neural networks.

2.4 Post-Quantum Security

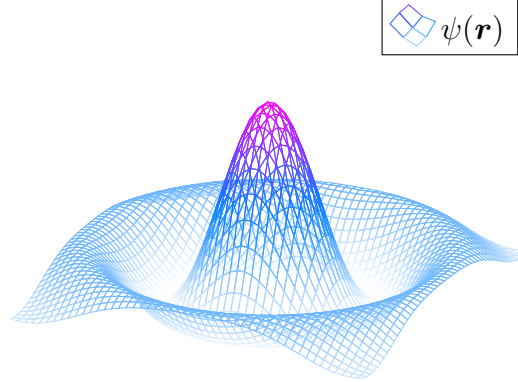


Figure 2.5: Illustration of a wave function ψ as commonly used in quantum mechanics. Its absolute value $|\psi(\mathbf{r}, t)|^2 = (\psi^* \psi)(\mathbf{r}, t)$ is a measure of the probability that a particle is currently at position \mathbf{r} at time t .

In quantum mechanics, we seek a mathematical description of quantum phenomena, commonly building upon SCHRÖDINGER's formalisms based on wave functions and the basic postulates of quantum mechanics.

The mathematical foundation of quantum mechanics is deeply rooted in linear algebra and functional analysis. An important concept is that of function spaces and, especially, Hilbert spaces. Function spaces are a widely useful concept, polynomial rings are a great example too (confer [definition 2.1.7](#)). Wave functions $\psi : \mathbb{R}^3 \times \mathbb{R} \mapsto \mathbb{C}$ are usually chosen as elements of the \mathcal{L}^2 -space, the space of square-integrable¹ functions:

$$\mathcal{L}^2 := \left\{ \psi : \mathbb{R}^3 \times \mathbb{R} \mapsto \mathbb{C} \mid \|\psi\| < \infty \right\} \quad \text{with } \|\psi\| := \int_{\mathbb{R}^3} d^3r \int_{\mathbb{R}} dt \, \psi^*(\mathbf{r}, t) \psi(\mathbf{r}, t)$$

with $\|\psi\|$ referred to as the l_2 -norm of the function ψ . By far not all functions are square integrable though, especially polynomials do not decrease in their absolute value towards $-\infty$ or ∞ , leading to $\|\psi\| \rightarrow \infty$, they are clearly not square integrable. An example that does work would be a normal distribution, or any function of the SCHWARTZ space.

The traditional Copenhagen interpretation relates a wave function to the probability that a particle is at the current position \mathbf{r} at time t at the given time. Namely, this probability is given by $|\psi(\mathbf{r}, t)|^2$, see [figure 2.5](#) for an exemplary illustration. The square-integrability requirement is imposed on the wave function ψ in order to make it normalizable, i.e. ensure that the total probability of presence is finite (or exactly 1) when integrated over all possible states the system might be in.

When describing a quantum particle or system, physicists usually work with mathematical objects in three different spaces:

- Position space inhabited by the wave function $\psi(\mathbf{r}, t) := \langle r | s_1, s_2, \dots, s_n \rangle \in \mathcal{L}^2$ (a function space),

¹Mathematicians usually formalise these using LEBESGUE-integrals instead of the commonly used RIEMANN formulation of an integral. LEBESGUE integration allows for a much broader class of integrable functions and is usually the preferred method in this context.

- Momentum space given by the Fourier-transformed wave function $\bar{\psi}(\mathbf{p}, t) := \langle p | s_1, s_2, \dots, s_n \rangle \in \mathcal{L}^2$ (also a function space) and
- State space, encompassing all possible basis states in which a system might currently be, a description that is usually highly specific to the problem we aim to solve with it. In the discrete, finite-dimensional case, represented by $|s_1, s_2, \dots, s_n\rangle \in \mathbb{S}$.

The electrons orbiting an atomic nucleus for instance, can be uniquely described by four quantum numbers (and corresponding Hermitian operators) forming a discrete state space: n, l, m_l and m_s with wave function $\langle r | n, l, m_l, m_s \rangle$ and momentum function $\langle p | n, l, m_l, m_s \rangle$.

Consider the following system of two base states $|0\rangle$ and $|1\rangle$, together forming an orthonormal basis. Due to *Quantum Superposition*, the measured system can be in any linear combination of the two,

$$|Q\rangle = \alpha |0\rangle + \beta |1\rangle, \quad \alpha, \beta \in \mathbb{C},$$

while enforcing that the scalar product of $\langle Q |$ with $|Q\rangle$ is normalized to 1 by the second axiom of probability theory, i.e.

$$\langle Q | Q \rangle = (\alpha^* \langle 0 | + \beta^* \langle 1 |) (\alpha |0\rangle + \beta |1\rangle) = |\alpha|^2 + |\beta|^2 \stackrel{!}{=} 1.$$

Here we use that $\{|0\rangle, |1\rangle\}$ comprise an orthonormal basis and therefore $\langle 0 | 1 \rangle = 0$, $\langle 1 | 0 \rangle = 0$, $\langle 0 | 0 \rangle = 1$ and $\langle 1 | 1 \rangle = 1$. This seemingly simple system is referred to as a *Qubit*, the basic unit of quantum information theory, uniquely represented by α and β .

Said to be 'at the heart of the disparity between classical and quantum physics', *Quantum Entanglement*, which Einstein once referred to as "spooky action at a distance", breaks the physical principle of locality but is yet a fundamental part of most quantum theories (Bell, Horne and Zeilinger 1989). This phenomenon describes the connection between two or more quantum particles related to each other through the mutual dependence of their quantum states $|s_1, s_2, \dots, s_n\rangle$. Phrased differently, their states cannot be described independently of the rest of the particle group. For instance, two antisymmetrically entangled fermions never expose the same spin when measured simultaneously, even when they are far apart from each other - this has also been shown experimentally (Yin et al. 2013).

Quantum computers exploit the physical properties of quantum systems such as superposition and entanglement in order to speed up computations. They facilitate up to exponential speedups when algorithms are available, compared to problems on traditional computers. In conventional complexity theory, problems are filed into different complexity classes when analysing their runtime and memory usage. There exist

1. NL (Nondeterministic Logarithmic space)
2. P (Polynomial time)
3. NP (Nondeterministic Polynomial time)
4. PSPACE (Polynomial space)
5. EXPTIME (Exponential time)
6. EXPSPACE (Exponential space)

computational complexity classes, sorted by the amount of problems contained in them ($NL \subseteq P \subseteq NP \subseteq PSPACE \subseteq EXPTIME \subseteq EXPSPACE$). A particularly interesting open problem is whether $P = NP$, one of the millennium prize problems. The **NP** class of problems is particularly useful in cryptography, it is especially important for the hardness assumptions of cryptographic schemes, problems should be at least as hard as the hardest problems in **NP**.

2.4.1 Definition: NP-Hardness

A problem is referred to as *NP-hard* iff it is at least as hard as the hardest problems in the complexity class **NP** (nondeterministic polynomial time). Formally written,

$$\mathbf{NP} := \bigcup_{k \in \mathbb{N}} \mathbf{NTIME}(n^k)$$

the union of all decision problems with runtime bounded by $\mathcal{O}(n^k)$.

One of the first major algorithms in this context is SHOR's algorithm, discovered before the first working quantum computer was built.

2.4.1 Shor's Algorithm

In the **RSA** scheme, but also other cryptographic schemes, the whole scheme's security is based on the hardness assumption of the integer factorisation problem. As of today, the cryptographic community still lacks a proof that the factorisation problem is in **NP**, yet it is widely believed to be. What we do know however, is that **RSA** encryptions can be broken and signatures forged, as soon as a sufficiently powerful quantum computer (with enough Qubits of memory) is built, in part explaining the global interest of governments and security organisations in the topic. **Discrete Logarithm Problem (DLP)**-based systems such as the **DIFFIE-HELLMAN** key exchange are also affected.

The algorithm enabling this was invented by Peter SHOR in 1994 and will be outlined here shortly as it is a core element to security considerations of modern cryptosystems. The core structure of the algorithm is

1. guessing some $g \in \mathbb{N}$ that we hope shares a factor with a large $N = p \cdot q$ ($p, q, N \in \mathbb{N}$),
2. improving that guess g by a quantum subroutine and
3. applying EUCLID's algorithm to find p and q the factors of N .

As soon as we found a guess g that satisfies $\gcd(N, g) \neq 1$, the algorithm finishes and we are done (Shor 1997).

The core factorisation idea is the following, not specific to quantum computation: We know that for a pair $g, N \in \mathbb{N}$, we can always find some $r \in \mathbb{N}$ such that

$$g^r = mN + 1, \quad m \in \mathbb{N},$$

we are looking for a g^r that is exactly one more than a multiple of N . Rearranging,

$$g^r - 1 = mN \iff (g^{\frac{r}{2}} + 1)(g^{\frac{r}{2}} - 1) = mN$$

we have found two factors $g^{\frac{r}{2}} + 1$ and $g^{\frac{r}{2}} - 1$ (for even r) that share a common factor with N and apply Euclid's algorithm to get p and q . These two factors $g^{\frac{r}{2}} + 1, g^{\frac{r}{2}} - 1$ might themselves be multiples of N , or r might be odd, rendering the guess useless and we need to start over with a new $g \in \mathbb{N}$. According to Shor 1997, we find 'good' factors roughly 35.7 % of the time with just one guess, with only ten tries we arrive at a success rate > 99 %. The plain guessing process can be done by any common computer, but is even more inefficient for large N (and resulting large r) than just factoring N using a general number field sieve (the state-of-the-art method of plain factorisation).

This is where the quantum component comes in, efficiently *improving* the guess g , therefore finding r . Using a quantum superposition, a quantum computer can calculate the output of a function for multiple superpositioned inputs *simultaneously*, which is what makes them so incredibly fast in some applications. When measuring the output state, the key idea of a quantum computation is to arrange the inputs in such a way that only useful output remains, while the other terms cancel each other out by destructive interference.

Thereby, we instruct the quantum computer to raise our guess g by all possible powers $\in \mathbb{N}$ up to some boundary in order to obtain

$$|1, g^1\rangle + |2, g^2\rangle + |3, g^3\rangle, \dots$$

which we then take modulo N , resulting in a superposition of remainders

$$|1, [g^1]_N\rangle + |2, [g^2]_N\rangle + |3, [g^3]_N\rangle + \dots$$

Here is where SHOR's key idea came in: The remainders in the above superposition expose repetitions at a period of exactly r (which, by our definition fulfils $g^r \equiv 1 \pmod{N}$) because for any $a \in \mathbb{Z}$,

$$g^x \equiv g^{x+r} \equiv g^{x+2r} \equiv \dots \equiv g^{x+ar} \pmod{N}$$

the remainders are periodic with frequency $\frac{1}{r}$. The above can be quickly derived from $g^r = mN + 1$, therefore

$$g^{x+r} = g^x g^r = (\tilde{m}N + [g^x]_N)(mN + 1) = (m\tilde{m}N + [g^x]_N m + \tilde{m})N + [g^x]_N$$

is indeed congruent to $g^x \pmod{N}$.

And therefore, we can use a **Quantum Fourier Transform (QFT)**, discovered by Don Coppersmith in 1994, on the superposition of remainders of powers of g to find the period r which is exactly what we were looking for. From the output of

$$\text{QFT}\left(|1, [g^1]_N\rangle + |2, [g^2]_N\rangle + |3, [g^3]_N\rangle + \dots\right)$$

we obtain the dominant frequency $\frac{1}{r}$ yielding us our desired improved guess (Shor 1997). Which again, can be evaluated extremely quickly on the given superpositioned inputs using a quantum computer, at least in theory. From here, we obtain $g^{\frac{r}{2}} + 1$ and $g^{\frac{r}{2}} - 1$ in order to finally find the factors p and q of N using EUCLID's algorithm on $g^{\frac{r}{2}} \pm 1$ and N .

For large numbers N however, today's quantum computers' performance is still far off from factoring N into $p \cdot q$ effectively, for relatively small N however, it is already possible.

2.4.2 Outlook

Another important advancement in quantum computing related to cryptography is Grover's algorithm which provides an asymptotic quadratic speedup for performing function inversion (Grover 1996). It could be used to perform certain key recovery, collision or pre-image attacks on cryptographic schemes, essentially halving the bit security of many schemes (128 bit security would be reduced down to 64 bits), suggesting to double the involved key size bits in many encryption schemes in order to be safe against potential future quantum attacks.

Lattice-based cryptosystems are still safe against quantum computation, i.e. quantum computers have a negligible advantage compared to traditional computers when attempting to break lattice-based encryptions, performing key-recovery attacks, etc. Two of these schemes will be presented in the next chapter, in section 3.3 and section 3.4.

Chapter 3

Homomorphic Encryption

HE makes it possible to operate on data without knowing it. One can distinguish three flavors of it, Partial-, Somewhat-, Levelled- and Fully Homomorphic Encryption (FHE).

For FHE, there exist a few schemes in use today with existing implementations.

- BFV scheme for integer arithmetic (Fan and Vercauteren 2012; Brakerski 2012).
- BGV scheme for integer arithmetic (Brakerski, Gentry and Vaikuntanathan 2012).
- CKKS scheme for (complex) floating point arithmetic (Cheon et al. 2017).
- Fastest Homomorphic Encryption in the West (FHEW) scheme for Boolean circuit evaluation (Ducas and Micciancio 2015).
- Torus Fully Homomorphic Encryption (TFHE) scheme for Boolean circuit evaluation (Chillotti et al. 2019).

We will first introduce the BFV scheme (integer arithmetic) as it represents a fundamental building block behind CKKS. Due to the inherent applications, this thesis will focus on the CKKS scheme to perform homomorphic operations on (complex-valued) floating point numbers and vectors.

To alleviate upcoming notation, for two tuples (\cdot, \cdot) defined over the same ring, denote their element-wise addition as $(\cdot, \cdot) + (\cdot, \cdot)$, element-wise multiplication by a scalar u as $u \cdot (\cdot, \cdot)$ and element-wise rounding as $\lfloor (\cdot, \cdot) \rfloor$.

3.1 Homomorphic Encryption using RSA

In order to illustrate the basic idea behind HE, without distancing ourselves too far from the original goal of introducing basic HE operations used in practice, this short section aims to motivate the definition of ring homomorphisms (cf. definition 3.1.1) behind a cryptographic background.

With unpadded RSA (R. L. Rivest, Shamir and L. M. Adleman 1983), some arithmetic can be performed on the ciphertext - looking at the encrypted ciphertext $\mathcal{E} : \mathbb{Z}/q\mathbb{Z} \mapsto \mathbb{Z}/q\mathbb{Z}$, $\mathcal{E}(m) := m^r$

mod q ($r, q \in \mathbb{N}$) of the message $m_1, m_2 \in \mathbb{Z}/q\mathbb{Z}$ respectively, the following holds:

$$\begin{aligned}\mathcal{E}(m_1) \cdot \mathcal{E}(m_2) &\equiv (m_1)^r (m_2)^r \pmod{q} \\ &\equiv (m_1 m_2)^r \pmod{q} \\ &\equiv \mathcal{E}(m_1 \cdot m_2) \pmod{q}\end{aligned}$$

RSA encryption (even supporting an unbounded number of modular multiplications) therefore fulfils the properties of a multiplicative ring homomorphism, which in general terms is defined as follows:

3.1.1 Definition: Ring Homomorphism

Given two rings $(R, +, \cdot)$ and (S, \oplus, \otimes) , we call a mapping $\varphi : R \rightarrow S$ a ring homomorphism when it satisfies the following conditions:

$$\forall a, b \in R : \varphi(a + b) = \varphi(a) \oplus \varphi(b) \wedge \varphi(a \cdot b) = \varphi(a) \otimes \varphi(b)$$

As we can see, the term **Homomorphic Encryption** originates from the ability to perform computations on encrypted data while ensuring the same results are obtained when the same operations are applied to the original data.

3.2 Gentry’s FHE-Scheme and BGV

Homomorphic encryption was envisioned by [R. Rivest, L. Adleman and Dertouzos](#) as early as the 70s but remained a phantasm for almost three decades and was since referred to as the ‘holy grail’ of cryptography. The first fully homomorphic encryption scheme was introduced in Craig GENTRY’s PhD thesis, based on lattice problems ([Gentry 2009](#)). In earlier schemes, each **HE** operation increases noise, making it partially homomorphic instead of fully homomorphic encryption. GENTRY devised a technique called *bootstrapping* that evaluates the *decryption* circuit homomorphically and thereby resets the noise introduced by previous operations, enabling true fully homomorphic encryption (**FHE**). Follow-up schemes improved his blueprint, Gentry’s work is clearly a landmark achievement ([Micciancio 2010](#)).

[Brakerski, Gentry and Vaikuntanathan 2012](#) developed a generalisation of **RLWE** that enables interpolation between **LWE** and **RLWE**, allowing for many improvements on earlier schemes, though mainly relying on [Gentry 2009](#). The resulting scheme, referred to as **BGV**, allows for integer arithmetic (addition and multiplication on $\mathbb{Z}/q\mathbb{Z}$). It also employs a modulus reduction technique, greatly extending the homomorphic capacity to a broader class of homomorphic circuits. [Microsoft SEAL 4.0 2022](#) implements the scheme, enabled using `seal::scheme_type::bgv`.

using the above Python code. An example of an invalid subset T that does cover the whole original set \mathbb{Z}_d^* would be $T = \{1, 7, 9, 15\}$.

For the purposes of **CKKS**, we simply choose a global T that is constant for our encoding and decoding procedure and a given d . The inverse natural projection π^{-1} then uniquely constructs a vector in \mathbb{H} by filling in elements \bar{z}_j for $j \notin T$ into \mathbf{z} . For simplicity, we commonly choose T as the 'first half' of \mathbb{Z}_d^* when sorting in an ascending manner as it is always a valid choice ³.

3.4.3 Definition: Discretisation to an element of $\sigma(R)$

Using one of several round-off algorithms (cf. [Lyubashevsky, Peikert and Regev 2013](#)), given an element of \mathbb{H} , define a rounding operation $\rho^{-1} : \mathbb{H} \mapsto \sigma(R)$ that maps an $\mathbf{h} \in \mathbb{H}$ to its closest element in $\sigma(R) \subset \mathbb{H}$, also denoted as

$$\rho^{-1}(\mathbf{h}) := \lfloor \mathbf{h} \rfloor_{\sigma(R)}.$$

Further let $\rho_\delta^{-1}(\mathbf{h}) = \lfloor \delta \cdot \mathbf{h} \rfloor_{\sigma(R)}$ denote the same rounding operation but with prior scaling by a scalar factor δ . Note that ρ is given directly as the identity operation because all elements of its domain are already elements of its image. Similarly, $\rho_\delta(\mathbf{y}) = \delta^{-1} \cdot \mathbf{y}$.

Because it is not essential to understanding the encryption scheme, we will skip over concrete implementations of the rounding procedure ρ^{-1} . For choosing a *close* element $\mathbf{g} \in \mathbb{H}$, we must first introduce a sense of proximity, in this case done by the l_∞ -norm $\|\mathbf{g} - \mathbf{h}\|_\infty$ of the difference between $\mathbf{h} \in \mathbb{H}$ and \mathbf{g} .

All in all, $m = \text{CKKS.Encode}(\mathbf{z})$, $\mathbf{z} \in \mathbb{C}^{N/2}$ applies all inverse transformations π^{-1} (first), ρ^{-1} (second) and σ^{-1} (third) to an input vector \mathbf{z} in order to finally arrive at a plaintext polynomial $m \in R/q_L R$ (equally stated as $m \in \mathbb{Z}_{q_L}/(X^N + 1)$ as long as N is a power of 2). Although σ is defined over \mathcal{S} instead of \mathcal{R} , all elements of $\sigma(R)$ can indeed be mapped back to an element in R using σ^{-1} . Summarised,

$$\mathbb{C}^{N/2} \xrightarrow{\pi^{-1}} \mathbb{H} \xrightarrow{\rho^{-1}} \sigma(R) \xrightarrow{\sigma^{-1}} R.$$

The decoding procedure $\mathbf{z} = \text{CKKS.Decode}(m)$, $m \in R$ does the opposite to re-obtain the input vector $\mathbf{z} \in \mathbb{C}^{N/2}$.

It should also be noted that the encoding procedure represents an isometric ring isomorphism (a linear bijection that preserves distance) between its domain and image, as does the decoding procedure. This reflects in the observation that the plaintext sizes and errors are preserved under the transformations ([Cheon et al. 2017](#)).

³This can be seen from the coset $-1T$ which exactly equals the 'missing' half in \mathbb{Z}_d^* when the first half is covered by $1T = T = \{1, 3, 5, \dots, N-1\}$ since $-1T = \{-1, -3, -5, \dots, -(N-1)\} \equiv \{d-1, d-3, d-5, \dots, d-N+1\} \pmod{d}$ when d a power of 2. Then, $(1T) \cup (-1T) = \{1, 3, 5, \dots, N-1\} \cup \{d-1, d-3, d-5, \dots, d-N+1\} = \{1, 3, 5, \dots, N-1, N+1, \dots, d-5, d-3, d-1\} = \mathbb{Z}_d^*$.

3.4.2 Scheme Definition

The **CKKS** scheme is a tuple of algorithms, introduced in [definition 3.4.4](#). To summarise the occurring parameters and variables, a brief overview of all used symbols is provided in [table 3.2](#).

3.4.4 Definition: The CKKS Scheme

Define $R, R/q_L R$ as in [definition 3.3.1](#). Introduce three bounded discrete probability distributions χ_{key} , χ_{enc} and χ_{error} over $R/q_L R$.

CKKS.

- ParamGen**(λ) Choose parameters as defined above, given the security parameter λ and space modulus q_L , choose $d \in \mathbb{N}$ a power of 2, $P, h \in \mathbb{Z}$, $\sigma \in \mathbb{R}$ and initialize distributions χ_{key} , χ_{enc} and χ_{error} . $\rightarrow \mathbb{P}$
- KeyGen**(\mathbb{P}) Sample the secret key $s \leftarrow \chi_{key}$, $a \in R_{q_L}$ uniformly at random, $\mu \leftarrow \chi_{error}$ and obtain the public key $\mathbf{p} = (b, a)$ with $b = -a \cdot s + \mu$. Sample $a' \in R_{P \cdot q_L}$ uniformly at random, $\mu' \leftarrow \chi_{error}$ and obtain the evaluation key $\gamma = (b', a')$ with $b' = -a' \cdot s + \mu' + P s^2$. $\rightarrow \mathbf{p}, s, \gamma$
- Encode**(\mathbf{z}) For a given input vector \mathbf{z} , output $m = (\underline{\sigma}^{-1} \circ \underline{\rho}_\delta^{-1} \circ \underline{\pi}^{-1})(\mathbf{z}) = \underline{\sigma}^{-1}(\lfloor \delta \cdot \underline{\pi}^{-1}(\mathbf{z}) \rfloor_{\underline{\sigma}(R)}) \rightarrow m$
- Decode**(m) Decode plaintext m as $\mathbf{z} = (\underline{\pi} \circ \underline{\rho}_\delta \circ \underline{\sigma})(m) = (\underline{\pi} \circ \underline{\sigma})(\delta^{-1} m) \rightarrow \mathbf{z}$
- Encrypt**(\mathbf{p}, m) Let $(b, a) = \mathbf{p}$, $u \leftarrow \chi_{enc}$, $\mu_1, \mu_2 \leftarrow \chi_{error}$, then the ciphertext is $\mathbf{c} = u \cdot \mathbf{p} + (m + \mu_1, \mu_2) = (m + bu + \mu_1, au + \mu_2) \rightarrow \mathbf{c}$
- Decrypt**(s, \mathbf{c}) Decrypt the ciphertext $\mathbf{c} = (c_0, c_1)$ as $m = [c_0 + c_1 s]_{q_L} \rightarrow m$
- Add**($\mathbf{c}_1, \mathbf{c}_2$) Output $\mathbf{c}_3 = \mathbf{c}_1 + \mathbf{c}_2 \rightarrow \mathbf{c}_3$
- Mult**($\mathbf{c}_1, \mathbf{c}_2$) Output $\bar{\mathbf{c}} = (c_0^1 c_0^2, c_0^1 c_1^2 + c_1^1 c_0^2, c_1^1 c_1^2) \rightarrow \bar{\mathbf{c}}$
- ReLin**($\bar{\mathbf{c}}, \gamma$) Using the evaluation key γ , relinearise from $\bar{\mathbf{c}} = (c_0, c_1, c_2)$ to $\mathbf{c} = (c_0, c_1) + \lfloor P^{-1} c_2 \gamma \rfloor \rightarrow \mathbf{c}$
- ReScale**(\mathbf{c}) In order to rescale a ciphertext from level l_{old} to l_{new} , multiply by a factor $\frac{q_{l_{new}}}{q_{l_{old}}} \in \mathbb{Q}$ and round to the nearest element of $(R/q_{l_{new}} R) \times (R/q_{l_{new}} R)$: $\mathbf{c}_{new} = \left\lfloor \frac{q_{l_{new}}}{q_{l_{old}}} \mathbf{c} \right\rfloor \rightarrow \mathbf{c}_{new}$

(Cheon et al. 2017)

For more details on the probability distributions, refer to the original CKKS paper ([Cheon et al. 2017](#)), with the following naming relations: $\chi_{key} = \mathcal{HWT}(h)$ over $\{0, \pm 1\}^N$, $\chi_{error} = \mathcal{DG}(\sigma^2)$ over \mathbb{Z}^N and $\chi_{enc} = \mathcal{ZO}(0.5)$ another distribution over $\{0, \pm 1\}^N$.

Encryption, decryption, addition and multiplication work similarly as in [definition 3.3.1](#). Unlike **BFV** however, **CKKS** works with different moduli q_L at each level L . This also casts off the need for up- and downscaling by δ when multiplying ciphertexts. The **CKKS.ReLin** operation serves the same purpose as in **BFV**, the rescaling operation is new however and takes care of the scale management. **CKKS.ReScale** can be employed whenever we want to work with ciphertexts at different levels, modifying a given ciphertext to the scale of the other enables the other operations to work just as usual. [Figure 3.2](#) shows the extended course of action in **CKKS** with a preceding encoding and decoding step.

Table 3.2: Summary of the parameters and symbols in CKKS.

Symbol	Space	Explanation
λ	$\in \mathbb{R}$	Security parameter
d	$\in \mathbb{N}$	Index of the cyclotomic polynomial used in R
P	$\in \mathbb{Z}$	Factor used during relinearisation
h	$\in \mathbb{Z}$	Hamming weight of the secret key (used by χ_{key})
σ	$\in \mathbb{R}$	Standard deviation of the Gaussian χ_{error}
q_L	$\in \mathbb{N}$	Modulus of $R/q_L R$ at level L
δ	$\in \mathbb{N}$	Scaling factor used when encoding
δ^{-1}	$\in \mathbb{R}$	Inversion coefficient of the effect of δ
s	$\in \{0, \pm 1\}^N$	Secret Key
\mathbf{p}	$\in (R/q_L R)^2$	Public Key (b, a)
γ	$\in (R/(Pq_L R))^2$	Relinearisation Key
\mathbf{z}	$\in \mathbb{C}^{N/2}$	Plain input vector
m	$\in R$	Plaintext Message
\mathbf{c}	$\in (R/q_L R)^2$	Ciphertext Message
$\bar{\mathbf{c}}$	$\in (R/q_L R)^3$	Slightly larger ciphertext from multiplication

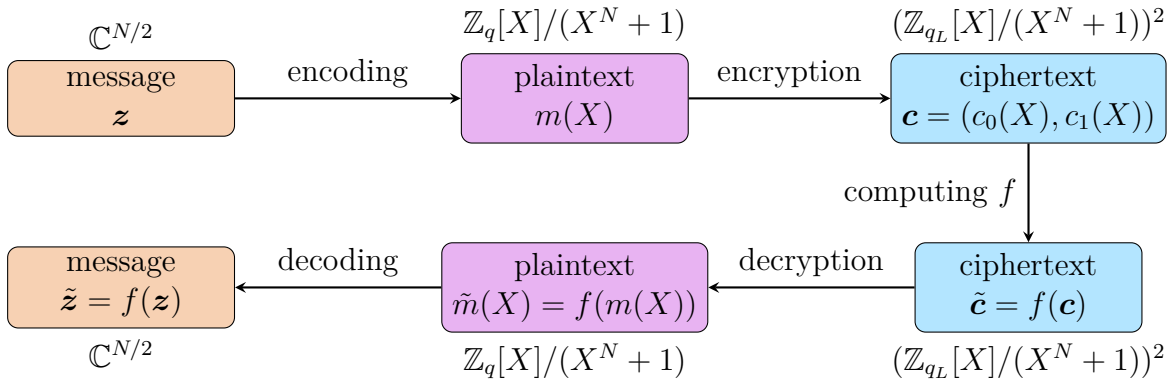


Figure 3.2: Schematic overview of CKKS, adapted from [Huynh 2020](#). A plain vector $\mathbf{z} \in \mathbb{C}^{N/2}$ is encoded to a plaintext polynomial $m = \text{CKKS.Encode}(\mathbf{z})$, encrypted to the ciphertext $\mathbf{c} = \text{CKKS.Encrypt}(\mathbf{p}, m)$ using the public key \mathbf{p} , operated on using a combination of $\text{CKKS}\{\text{Add}, \text{Mult}, \text{ReLin}, \text{ReScale}\}$ ciphertext operations and finally decrypted and decoded to a new $\tilde{\mathbf{z}} = \text{CKKS.Decode}(\text{CKKS.Decrypt}(s, \tilde{\mathbf{c}}))$ using the secret key s .

3.4.3 Verification of the Additive Homomorphism

3.4.1 Theorem: CKKS encryption is homomorphic with respect to addition

CKKS.Encode and CKKS.Encrypt should encrypt in such a way that the addition algebra can be retained even in the transformed space, showing that we can indeed refer to it as **homomorphic** encryption.

Proof. Similar to the BFV scheme proof ([theorem 3.3.1](#)), we aim to show that two input vectors $\mathbf{z}, \mathbf{z}' \in \mathbb{C}^{N/2}$ can be encoded, encrypted and added - and finally decrypted back to $\bar{\mathbf{z}} = \mathbf{z} + \mathbf{z}'$.

Due to the extremely high similarity of the BFV and CKKS schemes, they are even identical in their encryption, decryption and adding procedures, the only thing that remains to be shown is the additivity (or even linearity) of `CKKS.Encode`.

Encoding \mathbf{z} and \mathbf{z}' into m and m' , we obtain

$$m := \text{CKKS.Encode}(\mathbf{z}) = (\underline{\sigma}^{-1} \circ \underline{\rho}_\delta^{-1} \circ \underline{\pi}^{-1})(\mathbf{z})$$

comprised of three transformations $\underline{\sigma}^{-1}$, $\underline{\rho}_\delta^{-1}$ and $\underline{\pi}^{-1}$ which can be studied separately for their approximate additivity. If a function is linear and bijective (turning it into an isomorphism), its inverse will also be linear. We will utilize this below by only showing the additivity of $\underline{\sigma}$, $\underline{\rho}_\delta$ and $\underline{\pi}$, assuming their (approximate) bijectivity. Especially the bijectivity of $\underline{\sigma}$ is cumbersome to show and for more details we refer the reader to Cheon et al. 2017.

- The canonical embedding $\underline{\sigma}$ evaluates an input polynomial on the N^{th} roots of unity $\{\xi_j\}_{j \in \mathbb{Z}_d^*}$. For any two polynomials $p_1, p_2 \in \mathcal{S}$,

$$\underline{\sigma}(p_1 + p_2) = \left((p_1 + p_2)(\xi_j) \right)_{j \in \mathbb{Z}_d^*} = \left(p_1(\xi_j) + p_2(\xi_j) \right)_{j \in \mathbb{Z}_d^*} = \underline{\sigma}(p_1) + \underline{\sigma}(p_2).$$

- The rounding operation $\underline{\rho}_\delta^{-1}$ is only approximately additive due to its nature⁴. For any two vectors $\mathbf{h}_1, \mathbf{h}_2 \in \mathbb{H}$,

$$\begin{aligned} \underline{\rho}_\delta^{-1}(\mathbf{h}_1 + \mathbf{h}_2) &= \lfloor \delta \cdot (\mathbf{h}_1 + \mathbf{h}_2) \rfloor_{\underline{\sigma}(R)} = \lfloor \delta \mathbf{h}_1 + \delta \mathbf{h}_2 \rfloor_{\underline{\sigma}(R)} \approx \lfloor \delta \mathbf{h}_1 \rfloor_{\underline{\sigma}(R)} + \lfloor \delta \mathbf{h}_2 \rfloor_{\underline{\sigma}(R)} \\ &\approx \underline{\rho}_\delta^{-1}(\mathbf{h}_1) + \underline{\rho}_\delta^{-1}(\mathbf{h}_2). \end{aligned}$$

Its inverse $\underline{\rho}_\delta$ is fully additive nevertheless, since it acts as the identity (up to a scalar factor) of the subset $\underline{\sigma}(R)$ back to an element of \mathbb{H} .

- The natural projection $\underline{\pi}$ halves a vector in \mathbb{H} to an element of $\mathbb{C}^{N/2}$ which is naturally linear. Consider any $\mathbf{h}_1, \mathbf{h}_2 \in \mathbb{H}$, then

$$\underline{\pi}(\mathbf{h}_1 + \mathbf{h}_2) = (h_{1j} + h_{2j})_{j \in T} = (h_{1j})_{j \in T} + (h_{2j})_{j \in T} = \underline{\pi}(\mathbf{h}_1) + \underline{\pi}(\mathbf{h}_2).$$

As every step in the full encoding process $\underline{\sigma}^{-1} \circ \underline{\rho}_\delta^{-1} \circ \underline{\pi}^{-1}$ is additive, `CKKS.Encode` indeed acts additively. `CKKS.Decode` on the other hand is only approximately additive due to the rounding operation required in between.

The rest follows from [theorem 3.3.1](#) as encryption and addition of the BFV scheme are identical. All in all for `CKKS`, using the secret key s and public key \mathbf{p} ,

$$\text{Decode}(\text{Decrypt}(s, \text{Add}(\text{Encrypt}(\mathbf{p}, \text{Encode}(\mathbf{z})), \text{Encrypt}(\mathbf{p}, \text{Encode}(\mathbf{z}'))))) \approx \mathbf{z} + \mathbf{z}'.$$

We can conclude that encoding *and* encryption in CKKS are indeed homomorphic with respect to addition. \square

As the public key $\mathbf{p} = (b, a)$ corresponds to a sample from the RLWE distribution ([definition 2.2.8](#)), the implied security of the CKKS scheme is given by the hardness assumption of LWE ([theorem 2.2.1](#)). An attacker trying to decrypt a ciphertext \mathbf{c} , given only the public key \mathbf{p} , would thereby need to solve the RLWE search problem ([definition 2.2.9](#)) which is known to be hard (Lyubashevsky, Peikert and Regev 2010).

Microsoft SEAL 4.0 2022 implements the scheme, enabled using `seal::scheme_type::ckks`.

⁴For an illustrative counterexample of the additivity of rounding, refer to <https://math.stackexchange.com/questions/58239/linear-functions-with-rounding>.

Chapter 4

Implementation

4.1 Chosen Software Architecture

In the given setting, the most accessible frontend is commonly a JavaScript web application. A web-based demonstrator to show how to classify handwritten digits when using [homomorphic encryption](#) was implemented, comprised of a C++ server and a React¹ frontend, confer [figure 1.1](#).

To still make the classification run as quickly and efficiently as possible, a C++ binary runs in the backend providing an HTTP API to the frontend application. In order to allow for more flexibility of the HTTP server, the initial approach was to pipe requests through a dedicated web application framework with database access that would allow, for instance, user management next to the basic classification. However, the resulting communication and computation overhead, even when running with efficient protocols such as ZeroMQ, was too high.

Extending the accessibility argument to reproducibility, Docker is a solid choice ([Nüst et al. 2020](#)). The deployment is structured into two Docker images, *classifier* and *frontend*, easily scalable to multiple instance of the C++ upstream server using a round-robin load-balancing strategy of the single reverse proxy Nginx².

To run the attached demo project, simply execute

```
1 docker-compose build
2 docker-compose up
```

in the `code` folder and point your browser to <https://localhost>.

Using a Docker Multi-Stage Build, the application images were optimized towards a zero-dependency Alpine Linux image which contains nothing but compiled binaries and linked libraries. This is achieved by introducing intermediate layers including all necessary compiler libraries and dependencies and only copying the resulting binary to the final image. Similarly, the *frontend* build process of course requires Node JS, a common JavaScript engine used for the React compilation step, in a previous build layer. Yet, the final image only serves static files without any further server logic required and thus omits the entire JavaScript engine and associated libraries for the image. Details on the build process can be found in `code/classifier/classifier.Dockerfile` and `code/frontend/frontend.Dockerfile`.

¹<https://reactjs.org/>

²<http://nginx.org/>

4.2 The MNIST dataset

The **Modified National Institute of Standards and Technology (MNIST)** dataset of handwritten digits ([LeCun and Cortes 1998](#)) contains 60,000 train and 10,000 test images with corresponding labels. Some sample images are displayed in [figure 4.1](#), with ascending labels from 0 to 9. In order to stick to the traditional feedforward technique with data represented in vector format, therefore it is common to reshape data from (28, 28) images (represented as greyscale values in a matrix) into a 784 element vector.



Figure 4.1: Sample images of the MNIST dataset of handwritten digits ([LeCun and Cortes 1998](#)). The dataset contains 70,000 images of 28×28 greyscale pixels valued from 0 to 255 as well as associated labels (as required for supervised learning).

MNIST is one of the most commonly used datasets in **Machine Learning**, featured in an abundant number of tutorials and showcases, all in all it is fairly well studied. The National Institute of Standards and Technology recently published an extended version with uppercase and lowercase letters of the Latin alphabet contained as well (**EMNIST**), processed in the same way as **MNIST**, which should also work with our demonstrator.

4.3 Our Neural Network

The neural network implemented in our demonstrator was trained using the unencrypted standard **MNIST** dataset of 60,000 images, split into 90 % training and 10 % validation data. The training process itself was performed using the *Tensorflow* machine learning framework in Python³. The implemented network then has the following layer structure (also confer [figure 2.4](#)):

Layer 1: $\mathbf{h} = \text{relu_taylor}(M_1 \mathbf{x} + \mathbf{b}_1)$

Layer 2: $\mathbf{y} = \text{softmax}(M_2 \mathbf{h} + \mathbf{b}_2)$

Expressed in Python code, using the *Keras* extension of *Tensorflow*,

```

1 import tensorflow as tf
2
3 model = tf.keras.Sequential([
4     tf.keras.layers.Flatten(input_shape=(28, 28)),
5     tf.keras.layers.Dense(128, activation=relu_taylor),
6     tf.keras.layers.Dense(10),
7     tf.keras.layers.Activation(tf.keras.activations.softmax),
8 ])

```

³<https://www.tensorflow.org/>

For performance metrics and some statistical analysis of the network's accuracy, refer to [section 5.2](#).

To gain some intuition on what the two layers look like internally, the following plots of weights and biases have been made:

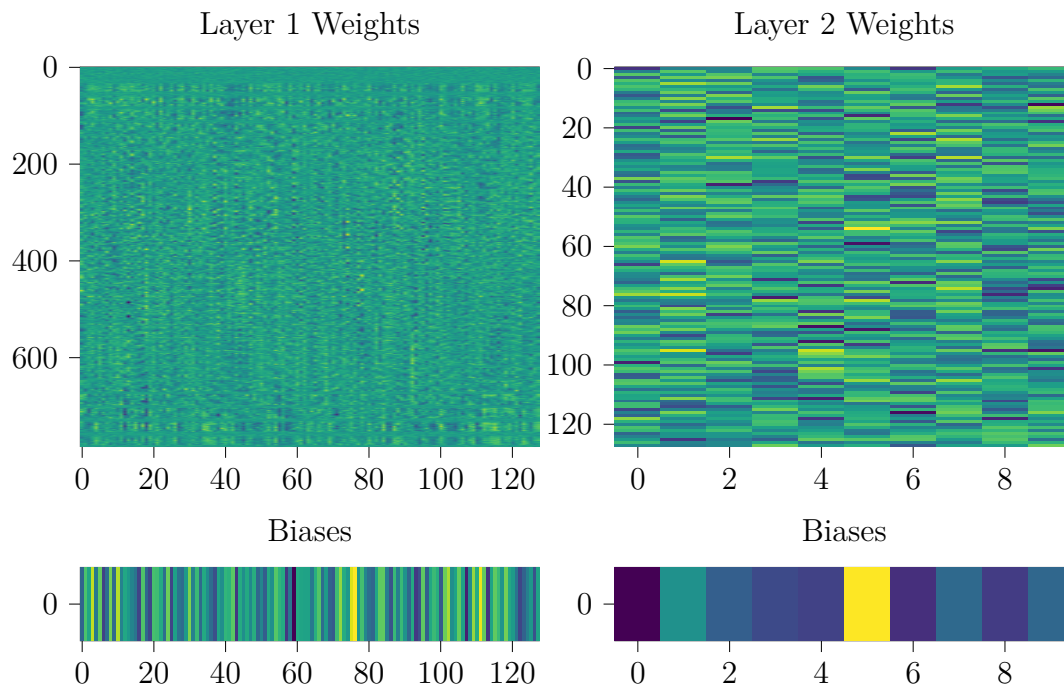


Figure 4.2: First and Second Layer Weights and Biases of the trained neural network. The weight matrices (784×128 and 128×10) are skewed to account for the different dimensions used. The biases have the same shape as the output of the matrix multiplication and the input of the next layer.

After going through both layers (confer [figure 4.2](#)), with the approximative `relu_taylor` activation function in between, the second (last) layer of the network outputs a vector of 10 scalars, each corresponding to one digit from 0 to 9. When finally applying the `softmax` function to the output, we can interpret the values as probabilities for each digit.

4.4 Matrix-Vector Multiplication

The dot product that is required as part of the neural network evaluation process needs to be implemented on **SEAL** ciphertexts as well.

There are multiple methods to achieve a syntactically correct dot product (matrix-vector multiplication) as described by [Juvekar, Vaikuntanathan and Chandrakasan \(2018\)](#) for (square) matrices.

1. **Naïve MatMul** - simple to derive but impractical in practice due to the limited further applicability of the result consisting of multiple ciphertexts. Applicable to arbitrary matrix dimensions, i.e. matrices $M \in \mathbb{R}^{s \times t}$, of course limited by the unreasonably high memory consumption and computation time of this approach.
2. **Diagonal MatMul** - a simple and practical solution applicable to square matrices $M \in \mathbb{R}^{t \times t}$ that has a major advantage compared to the previous method as the computation yields a single ciphertext object instead of many which can be directly passed on to a following evaluation operation.
3. **Hybrid MatMul** - essentially extending the diagonal method by generalising the definition of the diagonal extraction mechanism to 'wrap around' in order to match the dimensionality of the input vector. Applicable to arbitrary matrix dimensions, i.e. matrices $M \in \mathbb{R}^{s \times t}$ and favourable compared to the Naïve Method.
4. **Babystep-Giantstep MatMul** - a more sophisticated technique aiming to significantly reduce the number of Galois rotations as they are rather expensive to carry out, with a performance boost especially noticeable for higher matrix dimensions. Without further modification, applicable to square matrices.

For the following, define

$$\begin{aligned} \text{rot}_j : \mathbb{R}^t &\mapsto \mathbb{R}^t, \{\text{rot}_j(\mathbf{x})\}_i = x_{i+j} \\ \text{diag}_j : \mathbb{R}^{t \times t} &\mapsto \mathbb{R}^t, \{\text{diag}_j(M)\}_i = M_{i,(i+j)} \end{aligned}$$

with all indices $i, j \in \mathbb{Z}_t$ member of the cyclic quotient group $\mathbb{Z}_t := \mathbb{Z}/t\mathbb{Z}$ of all integers modulo t , meaning that overflowing indices simply wrap around again starting at index 0 to simplify notation. For the sake of compactness, we stick to this notation for the rest of the section.

4.4.1 The Naïve Method

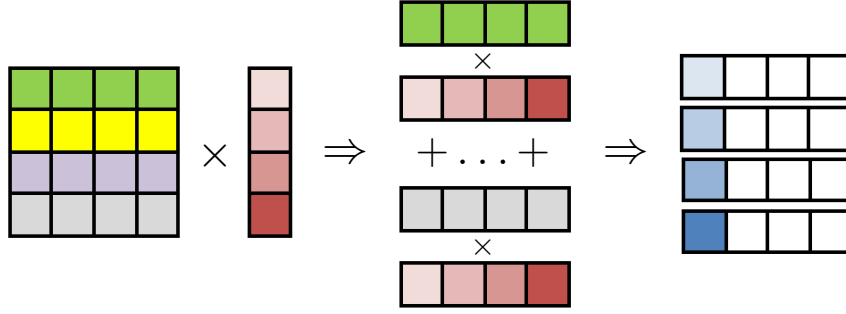


Figure 4.3: The naïve method to multiply a square matrix with a vector (adapted from Juvekar, Vaikuntanathan and Chandrakasan 2018).

Term by term, one can express a matrix-vector product of $M \in \mathbb{R}^{s \times t}$ and $\mathbf{x} \in \mathbb{R}^t$ as follows (also see figure 4.3):

$$\{M\mathbf{x}\}_i = \sum_{j=1}^t M_{ij}x_j.$$

Accordingly, a natural (or rather, naïve) way to model this multiplication in Microsoft SEAL would be to

1. encode each i -th matrix row ($M_{i,1}, M_{i,2}, \dots, M_{i,t}$) using the **Encoder** with matching parameters to the ciphertext of the encoded vector \mathbf{x} .
2. multiply each encoded row with the encrypted vector using `Evaluator.multiply_plain()` to obtain the ciphertext vector $\mathbf{y}_i \in \mathbb{R}^t$ for row i .
3. perform the 'rotate-and-sum' algorithm (Juvekar, Vaikuntanathan and Chandrakasan 2018) on each resulting vector (ciphertext) \mathbf{y}_i to obtain the actual dot product of the matrix row with the vector \mathbf{x} :
 - (a) using Galois automorphisms, rotate the entries of \mathbf{y}_i by $\frac{t}{2}$ elements to obtain $\text{rot}_{\frac{t}{2}}(\mathbf{y}_i)$.
 - (b) perform an element-wise sum $\mathbf{y}_i + \text{rot}_{\frac{t}{2}}(\mathbf{y}_i)$ whose first (and also second) half now contains the sum of the two halves of \mathbf{y}_i .
 - (c) repeat the previous two steps $\log_2(t)$ times, halving the split parameter t each time until one obtains 1 element, which yields us the requested sum of all entries $\sum_{k=1}^t \{\mathbf{y}_i\}_k$ as the dot product of \mathbf{x} and \mathbf{y}_i .
4. Given all the 'scalar' results of each row-vector dot product, we can construct the resulting matrix-vector product.

Adapting to non-square matrices The weight matrices in the given classification setting are not at all square, on the contrary their output dimension tends to be much lower than the input dimension as the overall goal is to reduce it from $28^2 = 784$ down to 10.

However, that also means one cannot directly apply the naïve or diagonal methods for multiplication. This 'flaw' can be mitigated by a simple zero-padding approach in order to make the matrix square, filling in zeroes until the lower-sized dimension reaches the higher one.

4.4.2 The Diagonal Method

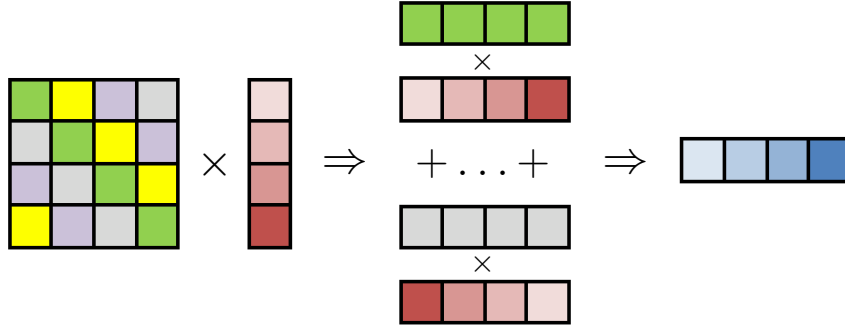


Figure 4.4: The diagonal method to multiply a square matrix with a vector (adapted from Juvekar, Vaikuntanathan and Chandrakasan 2018).

As can be seen in figure 4.4, we perform the vector-vector products over the diagonals of the matrix instead of the rows and rotate \mathbf{x} by one for each rotation.

4.4.1 Theorem: Diagonal Method

Given a matrix $M \in \mathbb{R}^{t \times t}$ and a vector $\mathbf{x} \in \mathbb{R}^t$, the dot product between the two can be expressed as

$$M\mathbf{x} = \sum_{j=0}^{t-1} \text{diag}_j(M) \cdot \text{rot}_j(\mathbf{x}).$$

Proof. For all indices $i \in \mathbb{Z}/t\mathbb{Z}$,

$$\left\{ \sum_{j=0}^{t-1} \text{diag}_j(M) \cdot \text{rot}_j(\mathbf{x}) \right\}_i = \sum_{j=0}^{t-1} M_{i,(i+j)} x_{i+j} \stackrel{[k=i+j]}{=} \sum_{k=i}^{t+i-1} M_{ik} x_k = \sum_{k=0}^{t-1} M_{ik} x_k = \{M\mathbf{x}\}_i.$$

□

The key idea of this optimization is to exploit the **Single Instruction Multiple Data (SIMD)** structure of the encryption schemes, in particular that of **CKKS**, and aggregating the result in one of the ciphertext objects.

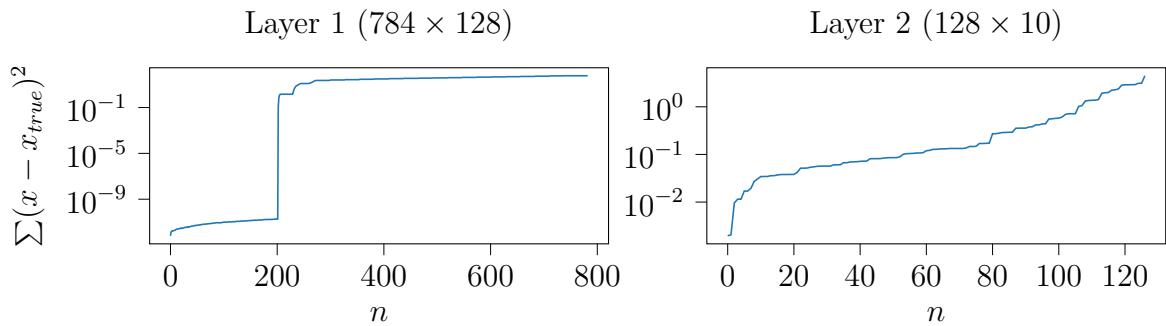


Figure 4.5: Diagonal Method error development after each rotation of the input vector.

One major problem of the diagonal method is that it requires many Galois rotations of \mathbf{x} , which is slow and also causes a large error after too many consecutive rotations (confer figure 4.5).

4.4.3 The Hybrid Method

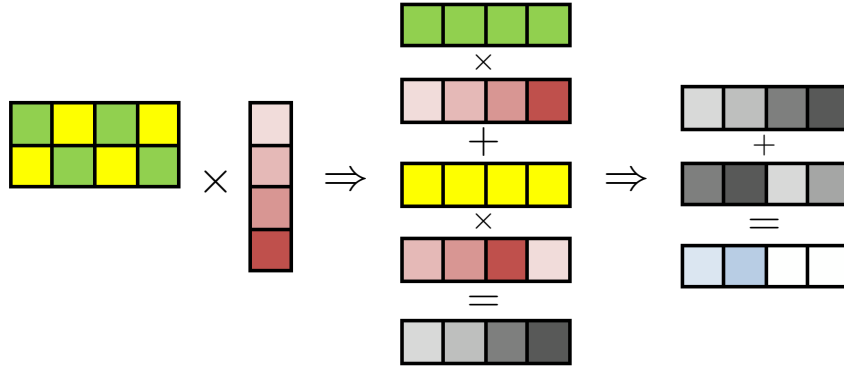


Figure 4.6: The hybrid method to multiply an arbitrarily sized matrix with a vector (adapted from [Juvekar, Vaikuntanathan and Chandrakasan 2018](#)).

To further extend the previous matrix multiplication method to solve the problem (cf. [section 4.4.1](#)), it is first necessary to extend the definition of the [diag](#) operator to non-square matrices $M \in \mathbb{R}^{s \times t}$. For the following, extending the above def:

$$\text{diag}_j : \mathbb{R}^{s \times t} \mapsto \mathbb{R}^t, \{\text{diag}_j(M)\}_i = M_{i,(i+j)}.$$

4.4.2 Theorem: Hybrid Method

For a matrix $M \in \mathbb{R}^{s \times t}$ with t a whole multiple of s and a vector $\mathbf{x} \in \mathbb{R}^t$,

$$M\mathbf{x} = (y_i)_{i \in \mathbb{Z}/s\mathbb{Z}} \text{ with } \mathbf{y} = \sum_{k=1}^{t/s} \text{rot}_{ks} \left(\sum_{j=1}^s \text{diag}_j(M) \cdot \text{rot}_j(\mathbf{x}) \right).$$

Proof. For all indices $i \in \mathbb{Z}/s\mathbb{Z}$,

$$\{\mathbf{y}\}_i = \left\{ \sum_{k=1}^{t/s} \text{rot}_{ks} \left(\sum_{j=1}^s \text{diag}_j(M) \cdot \text{rot}_j(\mathbf{x}) \right) \right\}_i = \sum_{k=1}^{t/s} \sum_{j=1}^s M_{i,(i+j)+ks} x_{(i+j)+ks},$$

substituting $l = i + j + ks$ and condensing the nested sums into one single summation expression since $\sum_{k=1}^{t/s} \sum_{j=1}^s f(j + ks) = \sum_{l=1}^t f(l)$, we obtain

$$y_i = \sum_{l=1+i}^{t+i} M_{il} x_l = \sum_{l=1}^t M_{il} x_l = \{M\mathbf{x}\}_i.$$

For a longer example on the index notation and derivation of the terms above including the condensed sum, refer to [appendix A.2](#). \square

Due to its low number of operations, the hybrid method almost always outperforms the naïve and diagonal methods ([Juvekar, Vaikuntanathan and Chandrakasan 2018](#)). A schematic representation illustrating the process can be seen in [figure 4.6](#).

To exemplarily discuss the implementation of an [HE](#) algorithm, we break down the following piece of code responsible for the hybrid matrix multiplication. Thanks to [SEAL](#)'s object-oriented

interface and explicit, consistent naming, the code snippets are mostly self-explanatory in combination with some additional comments.

We first encode the matrix diagonals using the `seal::CKKSEncoder` into a vector of plaintexts (each containing the information of one diagonal).

```

1 // diagonal method preparation
2 size_t in_dim = matrix.shape(0), out_dim = matrix.shape(1);
3 std::vector<seal::Plaintext> diagonals = encodeMatrixDiagonals(matrix,
  ↪ encoder, evaluator, in_out.parms_id(), in_out.scale(), nullptr, OUT_DIM);

```

Once this is done, we evaluate the inner sum $\sum_{j=1}^s \text{diag}_j(M) \cdot \text{rot}_j(\mathbf{x})$ using a loop.

```

1 // perform the actual multiplication
2 seal::Ciphertext sum = in_out; // makes a copy
3 evaluator.multiply_plain_inplace(sum, diagonals[0]); // performs the first
  ↪ vector-vector product
4 for (auto offset = 1ULL; offset < in_dim; offset++) {
5     seal::Ciphertext tmp; // for all remaining offsets:
6     evaluator.rotate_vector_inplace(in_out, 1, galois_keys);
7     evaluator.multiply_plain(in_out, diagonals[offset], tmp);
8     evaluator.add_inplace(sum, tmp);
9 }
10 in_out = sum; // and we arrive at the first result
11 evaluator.rescale_to_next_inplace(in_out); // scale down once

```

Finally, we exploit the repetitions in the resulting sum from above and rotate t/s times to end up with the sum of all chunks, encoded in one final ciphertext vector.

```

1 // perform the rotate-and-sum algorithm
2 seal::Ciphertext rotated = in_out; // makes a copy
3 for (size_t chunk = 0; chunk < in_dim / out_dim; chunk++) {
4     evaluator.rotate_vector_inplace(rotated, out_dim, galois_keys);
5     evaluator.add_inplace(in_out, rotated); // adds rotated result to itself
6 }
7 return in_out;

```

In the [Machine Learning](#) context, it is common to have a much higher input dimension than output dimension, usually leading to fully connected layers with matrices $M \in \mathbb{R}^{s \times t}$ with $s \ll t$. The hybrid method is especially efficient in these cases as it only requires $s + \frac{t}{s} = \frac{s^2+t}{s}$ rotations and s multiplications.

As outlined in [section 5.3](#), the hybrid method will prove to be the fastest method for the matrix sizes in our given project, with the 2nd best numerical accuracy.

4.4.4 The Babystep-Giantstep Method

Since Galois rotations are the most computationally intensive operations in most cryptographic schemes used today (Dobraunig et al. 2021), they take a large toll on the efficiency. In order to reduce the number of rotations required, one can make use of the Babystep-Giantstep (BSGS) optimisation as described in Halevi and Shoup 2018, which works as follows:

4.4.3 Theorem: Babystep-Giantstep Method

Given a matrix $M \in \mathbb{R}^{t \times t}$ and a vector $\mathbf{x} \in \mathbb{R}^t$, with $t = t_1 \cdot t_2$ split into two BSGS parameters $t_1, t_2 \in \mathbb{N}$ and

$$\text{diag}'_p(M) = \text{rot}_{-\lfloor p/t_1 \rfloor \cdot t_1}(\text{diag}_p(M)),$$

one can express a matrix-vector multiplication as follows:

$$M\mathbf{x} = \sum_{k=0}^{t_2-1} \text{rot}_{(kt_1)} \left(\sum_{j=0}^{t_1-1} \text{diag}'_{(kt_1+j)}(M) \cdot \text{rot}_j(\mathbf{x}) \right)$$

where \cdot denotes an element-wise multiplication of two vectors.

A proof of the above theorem can be found in appendix A.2.

Note that the optimized matrix-vector multiplication only requires $t_1 + t_2$ rotations as we can store the t_1 inner rotations of the vector \mathbf{x} for the upcoming evaluations. For larger matrices and vectors (larger t), $t_1 + t_2$ are indeed much smaller than the conventional number of required rotations $t = t_1 \cdot t_2$ in the diagonal method, or $\frac{s^2+t}{s}$ rotations in the hybrid method, which was the point of this modification in the first place. However, the number of multiplications and additions remains high - at least t multiplications are required, whereas the hybrid method only requires s multiplications (potentially much lower than t).

As we will see in section 5.3, the BSGS method also improves the performance of our classification process compared to the diagonal method, yet for the chosen parameters it does not reach the speed of the hybrid method. the approach of splitting the sum into two parts improves its performance close to that of the hybrid method.

4.5 Polynomial Evaluation

As the encryption hides the true value, we cannot directly evaluate the `relu` function since we have no way of telling whether it is larger than 0 or not. Using a finite series we can approximate the function though, also in the encrypted domain, because we can leverage the addition and multiplication operations of CKKS.

Finding a such approximation is not particularly hard, TAYLOR's theorem provides us with an explicit method to approximate a given analytic function in this way:

$$T_N f(x, x_0) := \sum_{n=0}^N \frac{f^{(n)}(x_0)}{n!} (x - x_0)^n$$

To accomplish the best possible result however, a CHEBYSHEV interpolation targeted at the corresponding domain subset may be a more suitable choice. Performing such an interpolation

on the interval $[-5, 10] \subset \mathbb{R}$ around 0 yields us the polynomial

$$\text{relu_taylor}(x) = -0.006137x^3 + 0.090189x^2 + 0.59579x + 0.54738$$

which is plotted next to the function it is supposed to interpolate in figure 4.7.

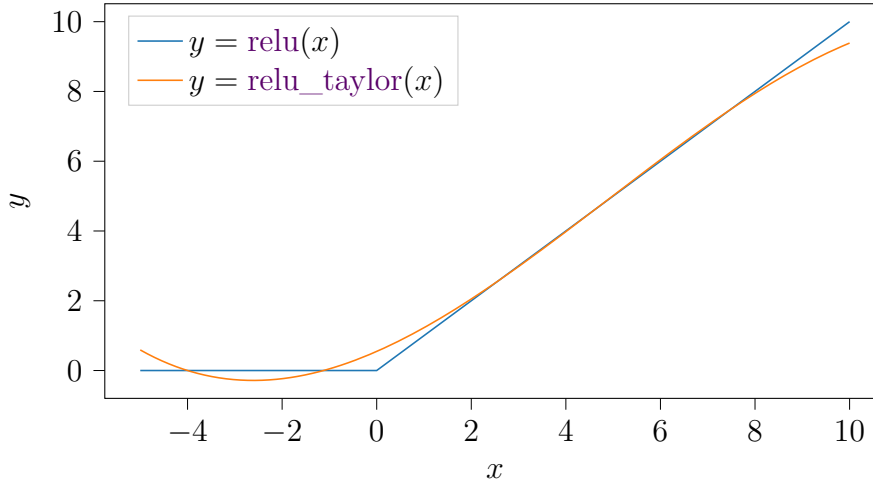


Figure 4.7: Comparison of the $\text{relu}(x)$ activation function vs. its series approximation $\text{relu_taylor}(x)$, plotted on the given domain. Outside of it, the two functions strongly disagree.

Next, we want to implement this polynomial evaluation using **SEAL**. From the implementation perspective, there are three properties to keep in mind when operating on a **SEAL** ciphertext (`seal::Ciphertext x`):

1. Scale (retrieved using `x.scale()`)
Can be adjusted with: `evaluator.rescale_inplace()`
2. Encryption Parameters (retrieved using `x.parms_id()`)
Can be adjusted with: `evaluator.mod_switch_to_inplace()`
3. Ciphertext Size (retrieved using `x.size()`)
Can be adjusted with: `evaluator.relinearize_inplace()`

For addition, the scales must be the same and they luckily will not change after the operation. The more delicate operation is ciphertext multiplication. Each time one multiplies two ciphertexts, the scales multiply (logarithmically, they add up, i.e. the common representations in bits are added together). The chain index reduces by 1, which for an encoded ciphertext depends on the coeff moduli. There must be enough bits remaining to perform the multiplication, namely $\log_2(\text{scale})$ bits.

To illustrate the connections of these properties to one another, the following explanation of Wei Dai, one of the maintainers of **SEAL**, on the "Scale out of bounds" error gives some good insight:

Scale has nothing to do with noise. "Scale out of bounds" can appear even if noise is extremely low. Although repeated multiplication of a ciphertext by a plaintext will slowly increase the noise, it is not the reason why you see "scale out of bounds".

The "Scale out of bounds" error specifically means that the scale of a ciphertext or plaintext is larger than the product of all elements in `coeff_modulus`. If you perform multiplications without rescaling, you can quickly see this error.

The more rescaling you perform, the less elements will be left in `coeff_modulus`. Even if you managed to have the same scale in a ciphertext after every multiplication and rescale, eventually the `coeff_modulus` can be too small to accommodate another multiplication (Dai 2020).

When evaluating a polynomial in SEAL, the above considerations need to be kept in mind when encoding the coefficients, multiplying the ciphertext \mathbf{x} with itself to reach higher powers and adding together the weighted monomials. We of course leverage the SIMD structure of the encryption scheme in order to turn the computation into an element-wise polynomial evaluation of the 1st layer’s output (an encrypted vector) before passing it on to the 2nd layer.

4.6 Further Implementation Challenges

When performing arbitrary computations on a ciphertext in SEAL, it is possible to encounter a *transparent ciphertext* from time to time. That is a ciphertext identically equal to 0 (mathematically, the tuple’s second polynomial is zero, confer definition 3.4.4), and it is usually not considered a valid encryption as anyone who has it can immediately ‘decrypt’ it to its underlying value of 0. However, for intermediate values of the computation at hand, forwarding values from addition to multiplication multiple times in our network, this is not an issue as long as we do not send the value back to the client, i.e. expose its internal structure (Laine 2020).

In our usual setting of a web-based demonstrator for recognising handwritten digits, this situation cannot be avoided - but as long as the client does not send a ciphertext identical to 0, our final classification result (a vector of 10 elements) will never be 0. Therefore, the server binary is compiled with the `-DSEAL_THROW_ON_TRANSPARENT_CIPHERTEXT=OFF` flag enabled, preventing a system halt in the case of an intermediary value evaluating to 0.

An important optimisation was to pre-encode the weight matrices and bias vectors upon startup of the server. This halved the individual request-response times, especially for the fast BSGS and hybrid methods.

The first layer multiplication is much slower than the second-layer one due to the large matrices, depending on the multiplication method, but around a factor of 60-100. For more details on runtime benchmarks, refer to section 5.3.

Chapter 5

Results

5.1 The Training Process

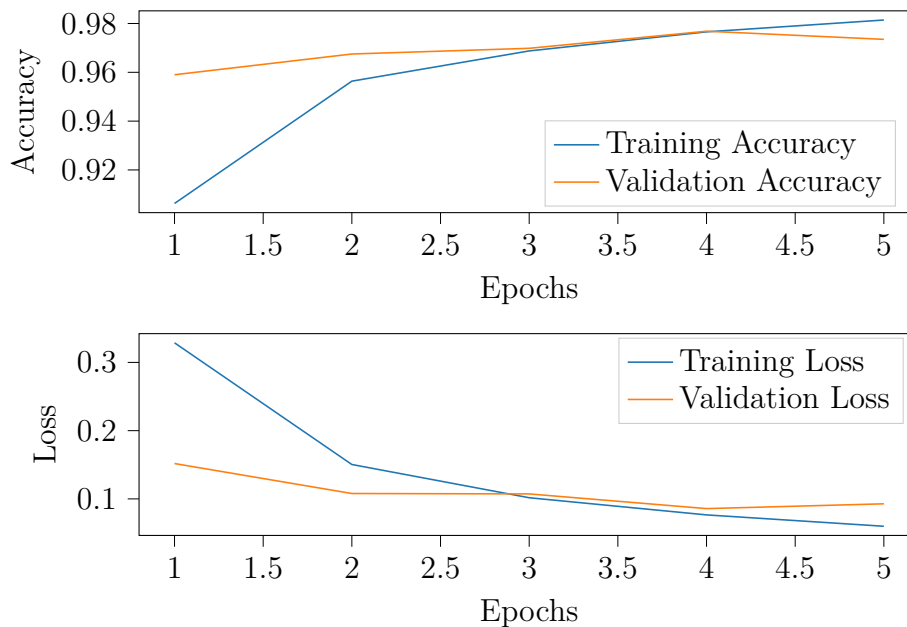


Figure 5.1: Development of the classification accuracy and the mean squared error during the training process of our neural network. Training and validation set metrics are plotted separately. When the validation accuracy starts to drop, the training process halts with the next epoch to prevent overfitting.

The machine learning framework behind the project, Tensorflow, splits its training process into *epochs*, which can be found on the x-axis in the plot above. For each training epoch, we find the progress that has been made in a single epoch by looking at the new accuracy (which percentage of the images has been classified correctly) and the loss function (MSE in this case). Per training run, we make a differentiation between training metrics and validation metrics, illustratively shown above for the given network. The validation data is not involved with the training process, it is only used to find a point in the process when training accuracy still rises while validation accuracy starts to drop (confer figure 5.1). At this point we will likely find the network’s learning process in an *overfitting* situation, so the training process terminates.

5.2 Accuracy, Precision, Recall

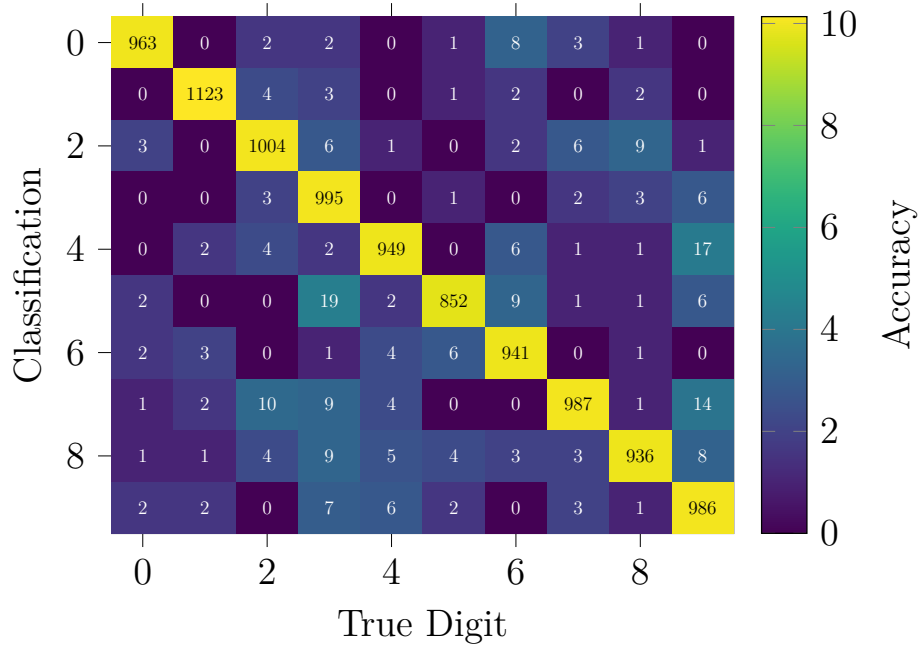


Figure 5.2: The Confusion Matrix of the trained network, showing digit-wise correct classifications in the diagonal and misclassifications, per digit-pair, in the off-diagonals. The matrix values were visually enhanced by mapping them to their logarithm base 2.

As we can see in figure 5.2, the majority of all images are classified correctly (visible in the diagonal). What makes the confusion matrix so interesting is identifying frequently mixed up digits, for instance, 3 and 5, 2 and 7 or 4 and 9. Judging with a human eye, this is somewhat reasonable, even more so when looking at the actual set of misclassified images (figure 5.3).



Figure 5.3: MNIST test images with true labels 0, 1, 2, 3, 4, 5, 6, 7, 8, 9 that were misclassified as 6, 8, 9, 8, 2, 6, 0, 9, 2, 3 by the neural network.

The plain network classifies 97.62 % of the 10,000 test images correctly. Running the encrypted classification on the full test set too, the encrypted network classifies 97.31 % of the test images correctly in $3\frac{1}{2}$ hours at full CPU utilisation, using the hybrid matrix multiplication method. For a binary classification, two further metrics of interest are

$$\text{Precision} := \frac{\text{tp}}{\text{tp} + \text{fp}} \quad \text{Recall} := \frac{\text{tp}}{\text{tp} + \text{fn}}$$

with tp ... True Positives, fp ... False Positives, fn ... False Negatives.

Precision (also referred to as PPV, positive predictive value) refers to the ability of the network to classify positive samples correctly, while Recall explains the completeness of the classified samples (i.e. how few true positives have been left out).

Table 5.1: Precision and Recall of the trained network for each digit individually, above for the plain network evaluation (P) and below for the encrypted evaluation (E).

Digit	0	1	2	3	4	5	6	7	8	9
Precision (P)	0.978	0.990	0.959	0.960	0.985	0.968	0.977	0.976	0.963	0.978
Recall (P)	0.986	0.989	0.975	0.977	0.975	0.964	0.980	0.964	0.967	0.955
Precision (E)	0.987	0.976	0.979	0.946	0.961	0.960	0.981	0.974	0.975	0.956
Recall (E)	0.989	0.990	0.958	0.981	0.975	0.966	0.972	0.963	0.937	0.959

Averaged over all digits, the mean precision (in plain) amounts to 97.37 % while the average recall is similarly high at 97.36 %. The encrypted network evaluation of the full test set yields an average Mean Max-Relative Error (see [table 5.2](#)) of 2.97 % using the hybrid method. And although it is numerically less accurate than the plain computation, only a handful of the 10,000 images were classified incorrectly, that the plain network managed to classify correctly.

5.3 Performance Benchmarks

This section finally gives a runtime and communication overhead analysis of the project. For fair comparisons, the preparations required for each method individually were not taken into account, as they can be performed once at the beginning of the program.

Table 5.2: Performance benchmarks and communication overhead of the classification procedure on an Intel® i7-5600U CPU, including the encoding and decoding steps. Different parameter sets B_1, B_2, N are compared for each of the implemented matrix multiplication methods *diagonal*, *hybrid* and *Babystep-Giantstep* (BSGS), looking at the averaged runtime, message size and also the accuracy when compared to the plain result (Δ).

B_1 ... Coefficient Moduli start bits (also equal to the last)

B_2 ... Coefficient Moduli middle bits, also defines the scale as 2^{B_2}

N ... Polynomial Modulus Degree, found in the exponent of $p(X) = X^N + 1$

T ... Runtime of encryption + classification + decryption

M ... Message Size (Relin Keys + Galois Keys + Request Ciphertext + Response Ciphertext)

Δ ... Mean Max-Relative Error compared to the exact result, i.e. $\Delta := \frac{\langle |y_{\text{prediction}} - y_{\text{exact}}| \rangle}{\max |y_{\text{exact}}|}$

Mode	SecLevel	B_1	B_2	N	MatMul	T / s	M / MiB	Δ / 1
Release	tc128	34	25	8192	Diagonal	8.39	132.72	0.0364
					Hybrid	1.35	132.72	0.0362
					BSGS	1.66	132.72	0.1433
	tc128	60	40	16384	Diagonal	17.24	286.51	0.0363
					Hybrid	3.05	286.51	0.0364
					BSGS	3.66	286.51	0.1399
	tc256	60	40	32768	Diagonal	35.24	615.16	0.0363
					Hybrid	5.99	615.16	0.0364
					BSGS	7.34	615.16	0.1399
Debug	tc128	34	25	8192	Diagonal	7.80	132.72	0.0358
					Hybrid	1.33	132.72	0.0370
					BSGS	1.66	132.72	0.1434

The above benchmarks (table 5.2) were accumulated on an Intel® i7-5600U CPU running at 2.6 GHz as the average over 3 individual runs with different test vectors, consistent across different parameter runs.

Without any encryption, the neural network classifies the full 10,000 image dataset in 515 ms on the same machine, as compared to $3\frac{1}{2}$ hours for the encrypted evaluation.

Obviously, smaller parameters B_1, B_2, N yield smaller polynomials, in the number of coefficients as well as the coefficient representations, and therefore cause less computation and communication overhead. The slowest method is the diagonal method, followed by BSGS and the winner is the hybrid method in this case, though not by far in terms of speed! Looking at accuracy, the diagonal method wins, although it is negligibly close to the numeric accuracy of the hybrid method.

The most secure tested parameters are 60, 40, 32768 which already lead to quite long classification times while ensuring a security level of 256 bits. For the web-based demonstrator (where speed matters), the natural choice is the first parameter set of 34, 25, 8192 which allows for the most efficient computations and short response times in combination with the hybrid matrix multiplication method, while still guaranteeing 128-bit security.

5.4 Ciphertext Visualisations

In order to visually demonstrate the encryption, visualisations of the ciphertext polynomial c_0 (refer to section 3.4) were generated using a decomposition of the Residue Number System (RNS) representation of c_0 . This is required because SEAL optimizes the storage of the ciphertext polynomials by splitting them up into sub-polynomials using the Chinese Remainder Theorem (CRT). The full modulus q , required to be huge for a secure system, is split up into multiple moduli q_1, q_2, \dots , depending on the system parameters, so that $q = q_1 \cdot q_2 \cdot \dots = \prod_{i=1} q_i$. Each pixel in the image below then corresponds to a coefficient $a \in \mathbb{Z}/q\mathbb{Z}$ scaled down by the total modulus q to obtain a brightness value between 0 and 1.

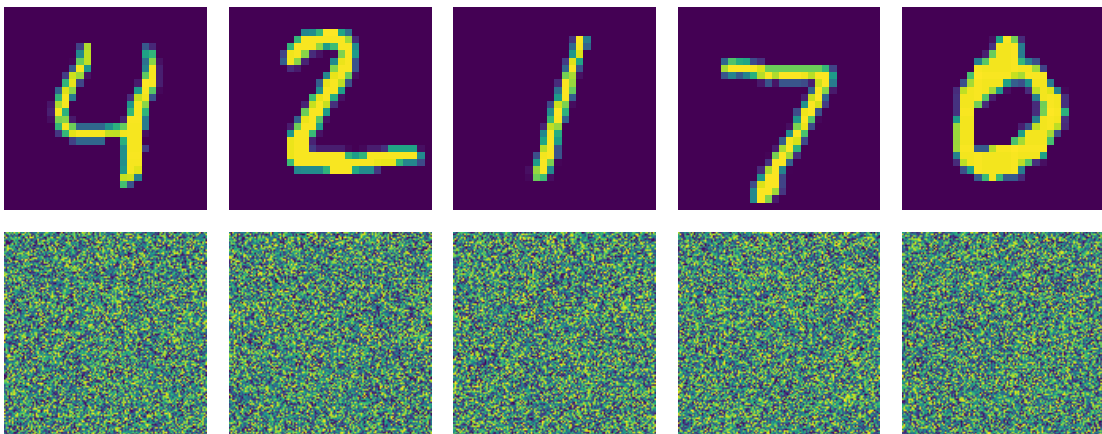


Figure 5.4: Ciphertext Visualisation: The first row corresponds to the images in plain, the second row depicts an encrypted version, namely the reconstructed polynomial coefficients a_k of the ciphertext polynomial.

Chapter 6

Conclusion

In the present thesis, we explored the interesting realm of homomorphic encryption in a machine-learning context while considering various security aspects of it. Next to the written part, the reader may find a server-client ('as a service') based demonstrator implementation of the homomorphically encrypted machine learning service for classifying handwritten digits, including a web-based frontend.

6.1 Summary

Chapter 2 introduced mathematical preliminaries of the lattice-based homomorphic encryption schemes used in chapter 3. As the focus lies on thoroughly understanding the notation used in the HE schemes, we first concentrated on the algebraic ring $\mathbb{Z}_q[X]/(X^N + 1)$ with integer coefficients modulo q and the cyclotomic polynomial $(X^N + 1)$ as its modulus. Forming the basis of the upcoming cryptographic schemes, we introduced the LWE problem and its descendant, RLWE. The multi-layered neural network is then trained using the backpropagation algorithm of the Tensorflow library, an approach similar to gradient descent - which was all introduced in the next section of chapter 2. The final section 2.4 introduced the reader to basic quantum mechanics and most of the necessary background to understand a simple quantum-mechanical system and the underlying principles of modern quantum computers.

Chapter 3 starts out with one of the first homomorphic schemes there is, unpadded RSA, motivating the need for such a structure. The first Fully Homomorphic Encryption scheme, invented by Craig GENTRY in his PhD thesis, strongly inspired further developments in the field: Based on lattice problems and the RLWE cryptosystem, Brakerski; Fan and Vercauteren introduced the BFV scheme for integer arithmetic. Extending it, we arrived at the CKKS scheme developed by Cheon et al. with an extensive encoding and decoding procedure. For both schemes, we verified the additive homomorphisms of the corresponding encryption (and encoding) operations `BFV.Encrypt` and `CKKS.Encrypt` \circ `CKKS.Encode`.

Chapter 4 then presents details about the implementation of the web-based demonstrator, concerning the deployment and software architectural specifics. The focus however lies on the technical challenges with Homomorphic Encryption in practice. Four different matrix multiplication techniques were introduced in detail, gradually increasing the complexity but also the efficiency. The next challenge ahead was evaluating the activation function in between the two layers, due to technical reasons, only approximated by a series expansion. As we further

found in [chapter 5](#), the most efficient multiplication method is the hybrid method. The results chapter presents the network's training results and a detailed statistical analysis of the network performance. To explicitly show the 'garbling' property of the encryption, the first polynomial of the ciphertext is visualised for a few test samples ([figure 5.4](#)). Finally, we analysed the runtime, network communication and numerical performance of the algorithms for different parameters, summarised in [table 5.2](#).

Two longer proofs were moved to [appendix A](#), one on the power-of-2 cyclotomic polynomials and a second one on the [BSGS](#) matrix multiplication method.

6.2 Related Works and Outlook

There are many existing approaches of [PPML](#) schemes or structures and even more applications - some related publications are, for the curious reader:

- CryptoNets (inferred [ML](#)), confer [Dowlin et al. 2016](#).
- Gazelle (inferred [ML](#)) as described by [Juvekar, Vaikuntanathan and Chandrakasan 2018](#).
- [TFHE](#) neural network inference, confer [Chillotti et al. 2019](#).
- Random Forests using [HE](#) as described by [Huynh 2020](#).
- Pasta for hybrid homomorphic encryption as described in [Dobraunig et al. 2021](#).

Next to Microsoft [SEAL](#), there are also other existing libraries for [HE](#):

- Microsoft's PyEVA, an interface to SEAL's CKKS implementation.
- Halevi & Shoup's HELib, a separate implementation of [HE](#) algorithms using NTL (the number theoretic library).
- Palisade, another collection of many implemented [HE](#) algorithms, supposed to be a general-purpose tool.
- TenSEAL from OpenMined, a high-level Python interface to SEAL.
- PyGrid and PySyft from OpenMined, libraries to publish encrypted learning data (PyGrid) and utilize it (PySyft) for [ML](#).

Considering the implications of mass surveillance and the thereby growing mindset for data privacy, the relevance of privacy-preserving/enhancing technologies will definitely grow in the coming years. The relatively new class of lattice cryptosystems looks immensely promising, given the interesting, especially useful properties of many such systems, and their inherent quantum security that will become even more relevant in the near future.

Acronyms, Definitions and Theorems

BFV	Brakerski-Fan-Vercauteren	2, 5
BGV	Brakerski-Gentry-Vaikuntanathan	5
BSGS	Babystep-Giantstep	44
CKKS	Cheon-Kim-Kim-Song	2, 5
CRT	Chinese Remainder Theorem	50
DFT	Discrete Fourier Transform	30
DLP	Discrete Logarithm Problem	23
FFT	Fast Fourier Transform	30
FHE	Fully Homomorphic Encryption	5, 25
FHEW	Fastest Homomorphic Encryption in the West	25
GapSVP	Decisional Approximate Shortest Vector Problem	14
GD	Gradient Descent	18
HE	Homomorphic Encryption	6
iff	if and only if	9
LWE	Learning With Errors	2, 13
ML	Machine Learning	7, 17
MNIST	Modified National Institute of Standards and Technology	6, 37
MSE	Mean-Squared-Error	17
NP	Non-deterministic Polynomial time	5
PPML	Privacy-Preserving Machine Learning	2
QFT	Quantum Fourier Transform	24
RLWE	Learning With Errors on Rings	13
RNS	Residue Number System	50
RSA	Rivest-Shamir-Adleman	5
SEAL	Simple Encrypted Arithmetic Library	2, 6
SIMD	Single Instruction Multiple Data	41
SIS	Shortest Integer Solution	14
TFHE	Torus Fully Homomorphic Encryption	25
TLS	Transport Layer Security	15

Definitions

2.1.1	Ring	7
2.1.2	Quotient Group / Ring	8
2.1.3	Polynomial Ring over \mathbb{Z}	9
2.1.4	Irreducible Polynomials	9
2.1.5	Cyclotomic Polynomial	11
2.1.6	Ring of Polynomials of highest degree $N - 1$	12
2.1.7	Polynomial Ring modulo q	12

2.2.1	Lattice	13
2.2.2	Shortest Vector Problem (SVP)	13
2.2.3	Decisional Approximate SVP (GapSVP)	14
2.2.4	Short Integer Solution (SIS) Problem	14
2.2.5	LWE-Distribution $A_{s, \chi_{error}}$	15
2.2.6	LWE-Problem - Search Version	15
2.2.7	LWE-Problem - Decision Version	15
2.2.8	RLWE-Distribution $B_{s, \chi_{error}}$	16
2.2.9	RLWE-Search Problem	16
2.2.10	RLWE-Decision Problem	16
2.3.1	Linear Regression	17
2.4.1	NP-Hardness	23
3.1.1	Ring Homomorphism	26
3.3.1	The BFV-Scheme	27
3.4.1	Canonical Embedding $\underline{\sigma}$	30
3.4.2	Natural Projection $\underline{\pi}$	31
3.4.3	Discretisation to an element of $\underline{\sigma}(R)$	32
3.4.4	The CKKS Scheme	33

Theorems

2.1.1	$2^{k\text{th}}$ Cyclotomic Polynomial	11
2.2.1	Hardness of LWE	15
2.3.1	Universal Approximation	20
3.3.1	BFV encryption is homomorphic with respect to addition	29
3.4.1	CKKS encryption is homomorphic with respect to addition	34
4.4.1	Diagonal Method	41
4.4.2	Hybrid Method	42
4.4.3	Babystep-Giantstep Method	44

Lemmata

2.1.1	Ring of Integers Modulo q : $\mathbb{Z}/q\mathbb{Z}$	8
2.1.2	The n^{th} roots of unity	10

Remarks

2.1.1	Irreducibility of Cyclotomic Polynomials	11
-------	--	----

Bibliography

- Ajtai, Miklós (1996). ‘Generating hard instances of lattice problems’. In: *STOC '96*.
- Bell, John Stewart, Michael A. Horne and Anton Zeilinger (1989). ‘Speakable and Unspeakable in Quantum Mechanics’. In: *American Journal of Physics* 57, pp. 567–567.
- Bishop, Christopher M. and Nasser M. Nasrabadi (2007). *Pattern Recognition and Machine Learning*. Vol. 16, p. 049901.
- Brakerski, Zvika (2012). ‘Fully Homomorphic Encryption without Modulus Switching from Classical GapSVP’. In: *IACR Cryptol. ePrint Arch.* 2012, p. 78. URL: https://link.springer.com/content/pdf/10.1007%2F978-3-642-32009-5_50.pdf.
- Brakerski, Zvika, Craig Gentry and Vinod Vaikuntanathan (2012). ‘(Leveled) fully homomorphic encryption without bootstrapping’. In: *ITCS '12*.
- Cheon, Jung Hee, Andrey Kim, Miran Kim and Yongsoo Song (2017). ‘Homomorphic Encryption for Arithmetic of Approximate Numbers’. In: *ASIACRYPT*.
- Chillotti, Ilaria, Nicolas Gama, Mariya Georgieva and Malika Izabachène (2019). ‘TFHE: Fast Fully Homomorphic Encryption Over the Torus’. In: *Journal of Cryptology* 33, pp. 34–91.
- Coppersmith, Don (1994). ‘An approximate Fourier transform useful in quantum factoring’. In: *IBM Research Report RC19642*.
- Corrigan-Gibbs, Henry, Sam Kim and David J. Wu (2018). *Lecture 9: Lattice Cryptography and the SIS Problem*. URL: <https://crypto.stanford.edu/cs355/18sp/lec9.pdf> (visited on 04/06/2022).
- Dai, Wei (18th June 2020). *Multiply plain repeatedly and scale out of bound error*. URL: <https://github.com/microsoft/SEAL/issues/182%5C#issuecomment-646234787> (visited on 20/04/2022).
- Dobraunig, Christoph, Lorenzo Grassi, Lukas Helming, Christian Rechberger, Markus Schafneger and Roman Walch (2021). ‘Pasta: A Case for Hybrid Homomorphic Encryption’. In: *IACR Cryptol. ePrint Arch.* 2021, p. 731.
- Dowlin, Nathan, Ran Gilad-Bachrach, Kim Laine, Kristin Lauter, Michael Naehrig and John Wernsing (Feb. 2016). ‘CryptoNets: Applying Neural Networks to Encrypted Data with High Throughput and Accuracy’. In: MSR-TR-2016-3. URL: <https://www.microsoft.com/en-us/research/publication/cryptonets-applying-neural-networks-to-encrypted-data-with-high-throughput-and-accuracy/>.
- Ducas, Léo and Daniele Micciancio (2015). ‘FHEW: Bootstrapping Homomorphic Encryption in Less Than a Second’. In: *EUROCRYPT*.
- Fan, Junfeng and Frederik Vercauteren (2012). ‘Somewhat Practical Fully Homomorphic Encryption’. In: <https://eprint.iacr.org/2012/144>. URL: <https://eprint.iacr.org/2012/144>.

- Gentry, Craig (2009). ‘Fully homomorphic encryption using ideal lattices’. In: *STOC ’09*.
- Goldwasser, Shafi (2018). ‘From Idea to Impact, the Crypto Story: What’s Next?’ In: URL: <https://www.youtube.com/watch?v=culuNbMPP0k> (visited on 01/03/2022).
- Grover, Lov K. (1996). *A fast quantum mechanical algorithm for database search*. DOI: [10.48550/ARXIV.QUANT-PH/9605043](https://doi.org/10.48550/ARXIV.QUANT-PH/9605043). URL: <https://arxiv.org/abs/quant-ph/9605043>.
- Halevi, Shai and Victor Shoup (2018). *Faster Homomorphic Linear Transformations in HElib*. Cryptology ePrint Archive, Report 2018/244. <https://ia.cr/2018/244>.
- Hornik, Kurt, Maxwell B. Stinchcombe and Halbert L. White (1989). ‘Multilayer feedforward networks are universal approximators’. In: *Neural Networks* 2, pp. 359–366.
- Huynh, Daniel (2020). ‘Cryptotree: fast and accurate predictions on encrypted structured data’. In: DOI: [10.48550/ARXIV.2006.08299](https://doi.org/10.48550/ARXIV.2006.08299). URL: <https://arxiv.org/abs/2006.08299>.
- Juvekar, Chiraag, Vinod Vaikuntanathan and Anantha P. Chandrakasan (2018). ‘Gazelle: A Low Latency Framework for Secure Neural Network Inference’. In: *CoRR* abs/1801.05507. arXiv: [1801.05507](https://arxiv.org/abs/1801.05507). URL: <http://arxiv.org/abs/1801.05507>.
- Kim, Andrey, Yuriy Polyakov and Vincent Zucca (2021). *Revisiting Homomorphic Encryption Schemes for Finite Fields*. Cryptology ePrint Archive, Paper 2021/204. <https://eprint.iacr.org/2021/204>. URL: <https://eprint.iacr.org/2021/204>.
- Laine, Kim (2020). *Result Ciphertext is Transparent*. GitHub. URL: <https://github.com/microsoft/SEAL/issues/224#issuecomment-702516479> (visited on 04/03/2022).
- LeCun, Yann and Corinna Cortes (1998). *The MNIST database of handwritten digits*. URL: <http://yann.lecun.com/exdb/mnist/>.
- Lepoint, Tancrede and Michael Naehrig (2014). ‘A Comparison of the Homomorphic Encryption Schemes FV and YASHE’. In: *AFRICACRYPT*.
- Lyubashevsky, Vadim, Chris Peikert and Oded Regev (2010). ‘On Ideal Lattices and Learning with Errors over Rings’. In: *EUROCRYPT*.
- (2013). ‘A Toolkit for Ring-LWE Cryptography’. In: *IACR Cryptol. ePrint Arch.*
- Mackay, David J. C. (2004). ‘Information Theory, Inference, and Learning Algorithms’. In: *IEEE Transactions on Information Theory* 50, pp. 2544–2545. URL: <http://www.inference.org.uk/itprnn/book.pdf> (visited on 17/07/2022).
- Micciancio, Daniele (2010). ‘A first glimpse of cryptography’s Holy Grail’. In: *Commun. ACM* 53, p. 96.
- Nüst, Daniel, Vanessa Sochat, Ben Marwick, Stephen J. Eglén, Tim Head, Tony Hirst and Benjamin D. Evans (2020). ‘Ten simple rules for writing Dockerfiles for reproducible data science’. In: *PLOS Computational Biology* 16.11, e1008316. DOI: [10.1371/journal.pcbi.1008316](https://doi.org/10.1371/journal.pcbi.1008316).
- Peikert, Chris (2016). ‘A Decade of Lattice Cryptography’. In: *IACR Cryptol. ePrint Arch.* 2015, p. 939.
- ProofWiki (2020). *Cyclotomic Polynomial of Index Power of Two*. URL: https://proofwiki.org/wiki/Cyclotomic_Polynomial_of_Index_Power_of_Two (visited on 06/06/2022).
- Regev, Oded (2005). ‘On lattices, learning with errors, random linear codes, and cryptography’. In: *STOC ’05*.
- (2010). ‘The learning with errors problem’. English (US). In: *Proceedings - 25th Annual IEEE Conference on Computational Complexity, CCC 2010*. Proceedings of the Annual IEEE

- Conference on Computational Complexity. 25th Annual IEEE Conference on Computational Complexity, CCC 2010 ; Conference date: 09-06-2010 Through 11-06-2010, pp. 191–204. ISBN: 9780769540603. DOI: [10.1109/CCC.2010.26](https://doi.org/10.1109/CCC.2010.26).
- Rescorla, Eric (2018). *The Transport Layer Security (TLS) Protocol Version 1.3*. RFC 8446. DOI: [10.17487/RFC8446](https://doi.org/10.17487/RFC8446). URL: <https://www.rfc-editor.org/info/rfc8446>.
- Rivest, Ronald, Leonard Adleman and Michael Dertouzos (1978). ‘On Data Banks And Privacy Homomorphisms’. In.
- Rivest, Ronald L, Adi Shamir and Leonard M Adleman (Sept. 1983). *Cryptographic communications system and method*. US Patent 4,405,829.
- Microsoft SEAL 4.0 (Mar. 2022). <https://github.com/Microsoft/SEAL>. Microsoft Research, Redmond, WA.
- Serge, Lang (2002). *Algebra*. 3rd ed. Springer. DOI: [10.1007/978-1-4613-0041-0](https://doi.org/10.1007/978-1-4613-0041-0).
- Shor, Peter W. (Oct. 1997). ‘Polynomial-Time Algorithms for Prime Factorization and Discrete Logarithms on a Quantum Computer’. In: *SIAM Journal on Computing* 26.5, pp. 1484–1509. DOI: [10.1137/s0097539795293172](https://doi.org/10.1137/s0097539795293172).
- StackExchange (2020). *Plot gradient descent*. user194703. URL: <https://tex.stackexchange.com/a/544832/155678> (visited on 07/07/2022).
- Yin, Juan, Yuan Cao, Hai-Lin Yong, Ji-Gang Ren, Hao Liang, Sheng-Kai Liao, Fei Zhou, Chang Liu, Yu-Ping Wu, Ge-Sheng Pan, Li Li, Nai-Le Liu, Qiang Zhang, Cheng-Zhi Peng and Jian-Wei Pan (June 2013). ‘Lower Bound on the Speed of Nonlocal Correlations without Locality and Measurement Choice Loopholes’. In: *Physical Review Letters* 110.26. DOI: [10.1103/physrevlett.110.260407](https://doi.org/10.1103/physrevlett.110.260407). URL: <https://doi.org/10.1103/2Fphysrevlett.110.260407>.

List of Figures and Tables

List of Figures

1.1	User interface of the demonstrator	6
2.1	The 5th roots of unity	10
2.2	Illustration of a standard lattice	14
2.3	Illustration of Gradient Descent	18
2.4	Neural Network illustration resembling the one used in our demonstrator	19
2.5	Illustration of a wave function	21
3.1	Schematic overview of the BFV scheme	28
3.2	Schematic overview of the CKKS scheme	34
4.1	Sample images of the MNIST dataset	37
4.2	Weights and biases of our neural network	38
4.3	Naïve matrix multiplication method	40
4.4	Diagonal matrix multiplication method	41
4.5	Error development after rotations of the diagonal method	41
4.6	Hybrid matrix multiplication method	42
4.7	Comparison of the Relu activation function vs. its Taylor expansion	45
5.1	Classification accuracy and loss development during training	47
5.2	Confusion Matrix of the trained network	48
5.3	Misclassified images of the test set	48
5.4	Visualisation of the plain input images compared to their ciphertext	50

List of Tables

3.1	Summary of the parameters and symbols in BFV	28
3.2	Summary of the parameters and symbols in CKKS	34
5.1	Precision and recall of each digit	49
5.2	Performance Benchmarks / Communication Overhead	49

Appendix A – Supplemental Proofs

A.1 Power-of-2 Cyclotomic Polynomials

Proof of [theorem 2.1.1](#). With $k \in \mathbb{N}$ a positive integer, we want to show that

$$\Phi_{2^k}(x) = x^{2^{k-1}} + 1.$$

A polynomial $p \in \mathbb{Z}[X]$ with

$$p(x) = x^n - a$$

of degree n has n roots

$$\{x_j\} = \{a^{\frac{1}{n}} e^{2\pi i \frac{j}{n}} \mid j \in \mathbb{N}, j \leq n\}$$

related by a factor $a^{\frac{1}{n}}$ to the n^{th} [roots of unity](#) given by powers of $\xi = e^{2\pi i \frac{1}{n}}$.

It is clear from the fundamental theorem of algebra that the polynomial p with roots $\{x_j\}$ can be factorised as

$$p(x) = \prod_{j=1}^n (x - x_j) = \prod_{j=1}^n (x - a^{\frac{1}{n}} e^{2\pi i \frac{j}{n}}).$$

Fixing $a = -1$, we obtain $p(x) = x^n + 1$ with roots given by

$$x_j = (-1)^{\frac{1}{n}} e^{2\pi i \frac{j}{n}} = (e^{i\pi})^{\frac{1}{n}} e^{2\pi i \frac{j}{n}} = e^{\frac{i\pi(2j+1)}{n}}$$

and according factorisation

$$p(x) = \prod_{j=1}^n (x - e^{\frac{i\pi}{n}(2j+1)}).$$

Further letting $n = 2^{k-1}$ and observing that

$$\gcd(2^k, l) = \begin{cases} 1 & \text{if } l \text{ odd} \\ 2 & \text{if } l \text{ even} \end{cases} \quad l, k \in \mathbb{N}$$

since a number 2^k that can only be decomposed into multiples of 2 never shares a factor with an odd number, in accordance with [lemma 2.1.2](#) we can conclude that the set of all odd roots of unity is exactly the set of all primitive roots (satisfying $\gcd(2^k, l) = 1$).

Following from above,

$$p(x) = \prod_{j=1}^{2^{k-1}} (x - e^{\frac{i\pi}{n}(2j+1)}) = \prod_{\substack{l=1 \\ l \text{ odd}}}^{2^k} (x - e^{\frac{i\pi}{n}l}) = \prod_{\substack{l=1 \\ \xi^l \text{ primitive}}}^{2^k} (x - \xi^l) = \Phi_{2^k}(x)$$

we arrive exactly at the definition of a cyclotomic polynomial ([definition 2.1.5](#)).
([ProofWiki 2020](#))

□

A.2 Babystep-Giantstep Multiplication

Proof of theorem 4.4.3. Starting from the adapted **BSGS** matrix-multiplication result $P = (P_1, P_2, \dots, P_t)^T \in \mathbb{R}^t$, we want to show that we indeed end up with an authentic matrix-vector product.

$$P_i := \left\{ \sum_{k=0}^{t_2-1} \text{rot}_{(kt_1)} \left(\sum_{j=0}^{t_1-1} \text{diag}'_{(kt_1+j)}(M) \cdot \text{rot}_j(\mathbf{x}) \right) \right\}_i = \sum_{k=0}^{t_2-1} \sum_{j=0}^{t_1-1} m'_{kt_1+j, (i+kt_1)+j} x_{(i+kt_1)+j}$$

with

$$m'_{p,i} = \left\{ \text{diag}'_p(M) \right\}_i = \left\{ \text{rot}_{-\lfloor p/t_1 \rfloor \cdot t_1} (\text{diag}_p(M)) \right\}_i = M_{i - \lfloor \frac{p}{t_1} \rfloor t_1, i - \lfloor \frac{p}{t_1} \rfloor t_1 + p}$$

and therefore

$$\begin{aligned} m'_{kt_1+j, i} &= M_{i - \lfloor \frac{kt_1+j}{t_1} \rfloor t_1, i - \lfloor \frac{kt_1+j}{t_1} \rfloor t_1 + kt_1 + j} \\ &= M_{i - kt_1 - \lfloor \frac{j}{t_1} \rfloor t_1, i - kt_1 - \lfloor \frac{j}{t_1} \rfloor t_1 + kt_1 + j} \\ &= M_{i - kt_1 - \lfloor \frac{j}{t_1} \rfloor t_1, i + j - \lfloor \frac{j}{t_1} \rfloor t_1} \\ m'_{kt_1+j, (i+kt_1)} &= M_{i+kt_1 - kt_1 - \lfloor \frac{j}{t_1} \rfloor t_1, i+kt_1 + j - \lfloor \frac{j}{t_1} \rfloor t_1} \\ &= M_{i - \lfloor \frac{j}{t_1} \rfloor t_1, i + kt_1 + j - \lfloor \frac{j}{t_1} \rfloor t_1} \end{aligned}$$

leading to

$$P_i = \sum_{k=0}^{t_2-1} \sum_{j=0}^{t_1-1} m'_{kt_1+j, (i+kt_1)+j} x_{(i+kt_1)+j} = \sum_{k=0}^{t_2-1} \sum_{j=0}^{t_1-1} M_{i - \lfloor \frac{j}{t_1} \rfloor t_1, i + kt_1 + j - \lfloor \frac{j}{t_1} \rfloor t_1} x_{(i+kt_1)+j}.$$

Noticing that the downward rounded fraction $\lfloor \frac{j}{t_1} \rfloor$ vanishes in a sum with j running from 0 to $t_1 - 1$, we can simplify to

$$P_i = \sum_{k=0}^{t_2-1} \sum_{j=0}^{t_1-1} M_{i, i+kt_1+j} x_{i+kt_1+j}$$

which contains two sums running to t_1 and t_2 respectively, containing an expression of the form $k \cdot t_1 + j$, which allows us to condense the nested sums into one single summation expression, as

$$\sum_{k=0}^{t_2-1} \sum_{j=0}^{t_1-1} f(kt_1 + j) = \sum_{l=0}^{t-1} f(l)$$

indeed catches every single value $l \in \{0, 1, 2, \dots, t-1 = t_1 \cdot t_2 - 1\}$ with $l = kt_1 + j$.

In summary, we obtain

$$\begin{aligned} P_i &= \sum_{k=0}^{t_2-1} \sum_{j=0}^{t_1-1} M_{i, i+kt_1+j} x_{i+kt_1+j} \\ &= \sum_{l=0}^{t-1} M_{i, i+l} x_{i+l} = \sum_{\nu=0}^{t-1} M_{i, \nu} x_{\nu} \\ &= \{M\mathbf{x}\}_i \end{aligned}$$

which indeed equals the conventional definition of a matrix-vector product. \square